HHS Public Access

A Review on Antibacterial Silk Fibroin-based Biomaterials: Current State and Prospects

Sama Ghalei[†], Hitesh Handa[†],*

[†]School of Chemical, Materials and Biomedical Engineering, University of Georgia, Athens 30602, United States

Abstract

Bacterial contamination of biomaterials is a common problem and a serious threat to human health worldwide. Therefore, the development of multifunctional biomaterials that possess antibacterial properties and can resist infection is a continual goal for biomedical applications. Silk fibroin (SF), approved by U.S. Food and Drug Administration (FDA) as a biomaterial, is one of the most widely studied natural polymers for biomedical applications due to its unique mechanical properties, biocompatibility, tunable biodegradation, and versatile material formats. In the last decade, many methods have been employed for the development of antibacterial SF-based biomaterials (SFBs) such as physical loading or chemical functionalization of SFBs with different antibacterial agents and bio-inspired surface modifications. In this review, we first describe the current understanding of the composition and structure-properties relationship of SF as a leading-edge biomaterial. Then we demonstrate the different antibacterial agents and methods implemented for the development of bactericidal SFBs, their mechanisms of action, and different applications. We briefly address their fabrication methods, advantages, and limitations, and finally discuss the emerging technologies and future trends in this research area.

Graphical Abstract

*Corresponding Author: Hitesh Handa, School of Chemical, Materials, and Biomedical Engineering, University of Georgia, 220 Riverbend Road, Athens, GA 30605, Telephone: (706) 542-8109, hhanda@uga.edu.

Declaration of interests

The authors declare that they have no known competing financial interests or personal relationships that could have appeared to influence the work reported in this paper.
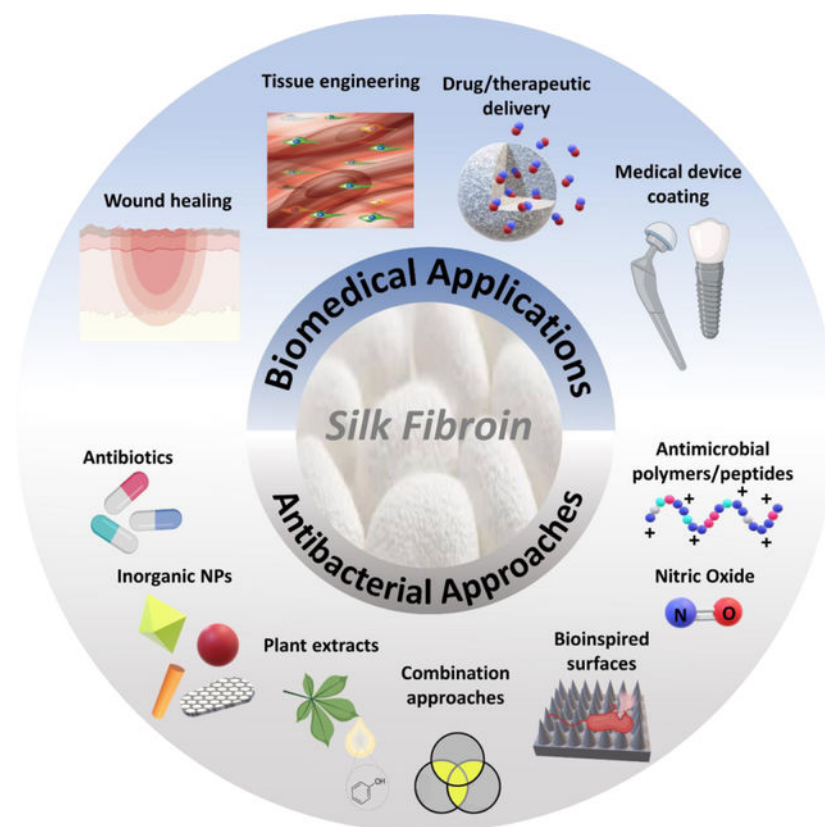
Keywords

1. Introduction

Silk fibroin is a natural macromolecular protein that has a long history of use in the textile industry and as a suture material in medicine [1]. Approved by the US Food and Drug Administration (FDA) as a biomaterial in 1993, SF has since been the subject of extensive research for different biomedical applications due to the unique combination of properties that it offers [2]. A high level of biocompatibility, tunable biodegradation, outstanding mechanical properties, processability into versatile material formats, and the presence of many accessible functional groups for chemical modifications have all rendered SF an extremely favorable material for development of various medical devices, drug delivery platforms, and tissue engineering scaffolds [3–5].

Silk is synthesized by the epithelial cells in specialized silk glands of different silkworms (mulberry and non-mulberry) and spiders [6]. The difference in silks obtained from various origins is mainly in their amino acid sequences and crystalline structure, giving rise to their distinct physical properties. While it is not feasible to obtain silk from spiders in large quantities [7], domesticated mulberry *Bombyx mori* (B. mori) silkworms provide a constant supply of silk that can be utilized in different fields [8]. Besides B. mori, silk

derived from other varieties of silkworms such as non-mulberry *Antheraea mylitta* (Indian Tasar silk), *Antheraea assama* (Indian Muga silk), *Antheraea pernyi* (Chinese Oak Tussah silk), *Antheraea yamamai* (Japanese silk) and *Philosamia ricini* (Indian Eri silk) have also recently found increasing interest due to their comparatively superior mechanical properties and performance [9]. However, owing to the difficulties associated with their extraction and processing, domesticated mulberry B. mori silkworms remain the primary source of silk for textile and biomedical applications [10].

The B. mori silkworm cocoons are mainly composed of silk fibroin (SF) fibers covered with an adhesive protein called sericin. Sericin is a hydrophilic polymer that holds the fibroin fibers together like a glue and accounts for almost 30% of the cocoon's weight [11]. Though individually investigated for biomedical applications, the combination of SF and sericin together in raw silk fibers has been rarely used due to the concerns raised regarding their adverse immune reactions and inflammatory activities. This was reported to be caused by the possible contamination from sericin and the wax like material present on the silk fibers [12]. Therefore, for most applications, the SF fibers are purified from sericin through a degumming process by boiling the cocoons in 0.02 M sodium carbonate solution based on a previously established extraction procedure [13]. According to the extraction protocol, the degummed SF fibers can be dissolved in 9.3 M lithium bromide solution and dialyzed against deionized water to obtain aqueous SF solution that can be further processed into many different material formats such as films, hydrogels, micro/nanoparticles, and micro/nanofibers. Other SF extraction methods based on proteolytic enzymes [14, 15], acid treatments [16], and low-pressure argon plasma [17] have also been reported. However, these methods have been less commonly utilized due their high cost and harsh effects on the structure and properties of SF fibers, respectively [18].

The B. mori SF is composed of a heavy (~350 kDa) and a light (~25 kDa) polypeptide chain (connected with a disulfide bond) along with the P25 glycoprotein in a molar ratio of 6:6:1 [19]. The heavy chain consists of repetitive hydrophobic domains, mainly composed of glycine, alanine, and serine amino acid sequences, and random hydrophilic domains consisting of acidic or charged amino acids such as glutamic acid, aspartic acid, arginine, and lysine [20]. The hydrophobic domains in SF can adopt a β-sheet conformation to form water insoluble crystalline regions that are responsible for the excellent mechanical strength of SF. These crystalline structures are interspersed between hydrophilic amorphous regions with α-helical conformation that provide SF with elasticity and toughness [21]. A schematic of the structure of silk fibroin is represented in Figure 1.

The superior mechanical properties of silk related to its molecular structure and packing, along with its high biocompatibility and tunable biodegradation have made SF distinctly unique among other natural and synthetic polymers [22]. The transformation of α-helical conformations into β-sheet crystalline structures in SF can be induced by different physical and chemical treatments *in vitro* to produce highly stable hydrogels and 3D scaffolds [23]. SF in an aqueous state or when dissolved in organic solvents (e.g., formic acid, hexafluoro-2-propanol) can also be used to fabricate films, nanofibers, and other type of biomaterials for different biomedical applications (Figure 2) [24, 25]. In addition, the presence of both hydrophilic and hydrophobic domains in the SF structure endows it with

a self-assembling ability in the aqueous environment, enabling the synthesis of SF micro/ nanospheres using water-based approaches [26]. SF-based micro/nanospheres have been widely investigated in the past for delivery of various drugs and therapeutic agents [27–29].

Despite the many outstanding properties of SF that qualifies it for a wide range of applications either alone or in combination with other biomaterials, a major limitation with SF biomaterials is the lack of inherent antibacterial activity. Bacterial infection is a great concern for indwelling medical devices and implantable biomaterials. Despite the standard sterilization treatments such as dry/wet heat or ionizing radiation, the surface of these materials can still be colonized by bacteria due to the possible contamination from the operating room environment, the patient's own skin, or other distal infections in the body [30, 31]. Biomaterial's contamination can give rise to difficult to treat infections that endanger the patient's life and put a burden on both the patient and healthcare budget by increasing the healing time and requiring a revision surgery to remove the infected implant [32]. In fact, biomaterial associated infections are one of the major reasons for failure of implants and medical devices. Health care-associated infections (HAIs) annually cost up to $33 billion and pose a severe threat to society [33]. Therefore, intensive efforts have been devoted to developing biomaterials that possess antibacterial activity and can resist such infections.

Due to the wide-ranging application of SF-based biomaterials (SFBs), over the last decade, many researchers have investigated different strategies to confer these materials with antibacterial properties. Various methods such as combination, modification, and functionalization with different antibacterial agents or alteration of the surface architecture have been implemented to prevent bacterial colonization on the surface of SFBs and improve their performance. In this review, for the first time we go through each of these methods, their advantages and drawbacks, and give an overview of the recent advances and future trend in this research area.

2.   SF interaction with bacteria

While the antibacterial applications of SFBs have been extensively explored in the past decade, the study of SF as a support material for bacterial adherence, growth, and biofilm formation is a newly emerged area of research that has found application in the fields of bioelectronics and bioanalytical sciences [34]. The as-spun silk fibers in the cocoons of silkworm larvae have been shown to provide a good substrate for the growth of various bacterial species and biofilm formation. The formed biofilm will in turn act as a primary defense barrier protecting the cocoon from environmental stresses. The *Pseudomonas cepacia* bacteria present in soil have also been found to feed on the carbon and nitrogen that they obtain by hydrolyzing the degummed silk via their fibrinase enzyme [35]. In a study by Tabei et al. SF films containing 0.5% glycerol as a plasticizer were demonstrated to have great ability to collect and retain a high density of various bacterial strains on their surface after a short period of exposure [36]. The attachment of bacteria to polymeric surfaces is governed by several factors such as surface hydrophobicity, surface charge, and surface chemical composition. While the mechanism of interaction of SF with bacteria and its supporting effect on biofilm formation has not yet been completely elucidated,

SF moderate wettability has been identified as one of the primary influential factors in the attachment of cells to its surface [37]. The initial bacterial adherence to a surface (docking stage) is determined by nonspecific cell-surface interactions such as van der Waals, electrostatic, and hydrophobic attractive or repulsive forces. The loosely attached bacteria to the surface then start to secret an extracellular polymeric substance (EPS) that allows for a stronger adhesion between bacteria and the surface (locking stage). SF protein with suitable hydrophobicity and excellent bioabsorbability has been demonstrated as an effective substrate for docking and immobilization of various bacterial species. Though favorable for some applications such as biofuels and microbial sensors [36], the supporting effect of SF in bacterial growth and proliferation is highly undesirable and must be avoided for medical devices and biomaterials related applications. In the next sections, we review on the different methods employed in the last decade to overcome the bacterial colonization of SFBs.

3. Antibacterial approaches for silk-fibroin based biomaterials

3.1 Antibiotics

Antibiotics are one of the most commonly used agents to be combined with SF-based biomaterials (SFBs) for prevention and treatment of bacterial infections. While systemic administration of antibiotics often results in poor tissue penetration and low bioavailability, and can cause adverse side effects, their localized delivery through implantable biomaterials and scaffolds offers several advantages. These advantages include tunable release directly at the site of infection and achieving a higher dosage with reduced side effects [38]. The release of antibiotics from SFBs can be controlled by tailoring their chemical and structural design as well as their biodegradation rate [39]. Since the bacteriostatic activity of such materials is dependent upon the release of an antibiotic from a silk fibroin-based substrate, most studies have implemented a zone of inhibition (ZOI) or disc diffusion test to evaluate the antibacterial responses (Table 1). ZOI test is a quick and rather inexpensive method that is used to determine the antibacterial activity of a material, in relation to a target microorganism, by measuring the size of the bacterial inhibition zone formed around the test material due to an antibacterial agent being released or leached out from it.

Depending on their type, antibiotics induce bacterial cell death through different approaches. For instance, aminoglycoside antibiotics (i. e. gentamicin) and tetracyclines are inhibitors of protein biosynthesis, quinolones such as levofloxacin and ciprofloxacin impede DNA replication, while glycopeptides (i. e. vancomycin) and β-lactam (i. e. amoxicillin) antibiotics interfere with normal bacterial cell wall synthesis [40]. In a study by Lan et al. vancomycin loaded gelatin microsphere were prepared and embedded in freeze-dried SF scaffolds for wound healing applications. According to a ZOI assay, the fabricated scaffolds were able to inhibit the gram-positive *Staphylococcus aureus* (*S. aureus*) while did not show any antibacterial activity against gram negative *Escherichia coli* (*E. coli*) bacteria after 24 h. This is because gram negative bacteria possess an outer membrane that makes them more resistant against β-lactam and glycopeptide antibiotics like vancomycin that act on the bacterial cell wall [41]. Therefore, for any application the choice of antibiotic is of primary importance and should be made based upon their mechanism of action and the type of target bacterial cells that they are going to counteract [42].

So far, many different antibiotic-loaded SFBs have been developed for versatile biomedical applications such as wound healing, bone tissue engineering, treatment of osteomyelitis, and development of sutures, ear tubes, and orthopedic implants (Table 1). Various physical and chemical methods have been implemented for fabrication of these antibiotic eluting SFBs. Antibiotics can be physically blended in SF aqueous/organic solutions prior to casting, electrospinning, and freeze-drying to obtain antibiotic loaded SF films [43, 44], electrospun fibers [45], or cryogels [41, 46, 47], respectively. In addition to physical approaches, the chemical surface modification of SFBs using plasma treatment has also been reported to be a viable method for conjugation of antibiotics to the surface of SFBs [48, 49]. Choudhury et al. developed amoxicillin trihydrate (AMOX) impregnated SF sutures using oxygen plasma treatment. According to their study, the oxygen plasma treatment of (*Antheraea assama*) silk fibroin (AASF) yarn resulted in the formation of a rougher morphology and oxygen containing functional groups on the surface, leading to an improved hydrophilicity and drug-impregnation efficiency by 16.7%. The oxygen plasma treated AASF/AMOX yarns (AASF/O_2/AMOX) had a sustained release of AMOX for up to 336 h and showed a clear ZOI against *S. aureus* (54.7 mm) and *E. coli* (19.3 mm) after 24 h *in vitro*. In addition, the *in vivo* analyses revealed the effectiveness of AASF/O_2/AMOX in mitigating the infection and reducing the healing time in an *S. aureus*-infected mouse wound model after 14 d. Other fabrication methods such as electrophoretic deposition of antibiotic loaded SF on the surface of metallic implants [50, 51], fabrication of layer by layer/coacervate antibiotic loaded coatings on SFBs (e. g. sutures) [52], and synthesis of composite SFBs using antibiotic loaded nanofillers [53] have also been described in the literature. In a recent study by Wu et al.[53], tetracycline hydrochloride (TCH) was first loaded into the lumen of halloysite nanotubes (HNTs) and then electrospun with SF aqueous solution to create antibacterial SF fibers. Compared to directly loading the TCH into SF fibers, the use of HNTs as an intermediary drug carrier resulted in a significantly more controlled release of TCH from SF fibers and therefore a longer lasting antibacterial effects against *S. aureus* and *E. coli* bacteria *in vitro* (Table 1).

Despite the ease of use, large availability, and low cost of antibiotics, the emergence of antibiotic-resistant bacteria over the past decades has hindered the application of antibiotic eluting SFBs. Biofilm formation on the surface of biomaterials and implants leads to development of resistant cells by providing an extracellular polymeric matrix composed of lipopolysaccharides, lipids, and proteins around the bacteria which protects them against the host immune system and antibiotics [54]. To eradicate the bacteria in biofilm and eliminate infection, remarkably higher drug doses and longer treatment periods are required compared to their free-living planktonic counterparts. This in turn prolongs and increases the patient's exposure to the drug, resulting in an enhanced risk of unwanted side effects [55].

Considering the inefficacy of the antibiotics in treatment of biofilm related infections, alternative approaches are essential to overcome the issues associated with bacterial resistance. In this regard, a fundamental understanding of antibiotics bactericidal mechanisms and drug-target interactions will be very helpful for development of new formulations and improvement of the old ones to increase their efficacy toward different types of bacteria.

3.2 Inorganic nanoparticles

Various inorganic nanomaterials with antibacterial properties such as metal (e. g. Ag, Au, Cu, Ca) and metal oxide nanoparticles (e. g. ZnO, TiO_2, CaO_2), transition metal dichalcogenide monolayers (e.g. $MoSe_2$), and graphene oxide (GO) nanosheets have been combined with SFBs for different biomedical applications (Table 2). Compared to antibiotics, it is more difficult for bacterial cells to develop resistance toward these nanomaterials due to their multiple mechanisms of action. The principal mechanism that inorganic nanomaterials employ to kill the invading bacteria is the generation of reactive oxygen species (ROS) [60]. ROS produced at low levels can be neutralized by bacterial cells antioxidant defense mechanisms. However, high concentrations of ROS can overcome these defense systems, causing oxidative damage to critical intracellular components such as enzymes, proteins, DNA, and lipids [61]. In addition to ROS generation, other bactericidal mechanisms of inorganic nanomaterials include disrupting the cell wall, damaging the chromosomes and DNA, and dysregulating the metabolic activity of the microorganisms [62].

Inorganic nanoparticles are typically synthesized using physiochemical approaches which are often costly and require the use of toxic substances and harsh conditions. Therefore, recently increasing attention has been given to simple and green methods of nanoparticles synthesis using biomaterials that are eco-friendlier and more biocompatible [63, 64]. SF is one of such materials that has been used frequently as a biocompatible reducing and stabilizing agent for *in situ* fabrication of various inorganic nanomaterials such as Ag NPs [65–67], Au NPs [68, 69], and CuBTC metal–organic framework (MOF) particles [70]. Being a protein, SF is mainly composed of repeated sequences of glycine, alanine, and serine amino acids with nearly 10% tyrosine residues evenly distributed throughout the protein sequence [71]. The ionization of tyrosine phenolic moiety at basic pH values and consequent electron transfer to the metal ions is recognized as the main mechanism of reduction by SF [72, 73]. Other reduction mechanisms such as chelation of metal ions and electron donation by unprotonated carboxylic groups at high pH [70] and reduction through the methanolic -OH groups in serine amino acids have also been reported by previous studies [74].

Moreover, the presence of hydrophilic–hydrophobic segments in the SF structure has been shown to facilitate its binding with inorganic NPs such as graphene and transition metal dichalcogenides (TMD) [75]. In a study by Huang et al. [76], carboxyl-modified silk fibroin (CMSF) was used as the exfoliating agent for preparation of $MoSe_2$ TMD nanosheets. The strong binding and interaction of CMSF carboxyl groups with the TMD atoms resulted in the formation of exfoliated $MoSe_2$ nanosheets with high efficiency and long-term dispersion stability. The $MoSe_2$–CMSF nanosheets exhibited good biocompatibility and high peroxidase-like catalytic activity toward the decomposition of H_2O_2 into •OH radicals therefore requiring the use of ~1000 times lower H_2O_2 dose for *in vitro* antibacterial effectiveness against gram-negative *E. coli* and gram-positive *Bacillus subtilis* (*B. subtilis*) bacteria compared to the traditional medical therapy. At physiologically relevant levels of H_2O_2, $MoSe_2$-based films were also shown to effectively promote the wound healing and prevent infections *in vivo* using Kunming mice with infected skin wounds as models.

In addition to *in situ* fabrication methods, antibacterial SFB composites containing inorganic nanomaterials can also be made *ex situ* by first synthesizing the nanoparticles and then incorporating them into the SFB substrate [77, 78]. Embedding inorganic nanoparticles in SFBs not only endow them with antibacterial activity and improve their mechanical properties but also prevents excessive NPs leaching, resulting in prolonged antibacterial longevity, reduced cytotoxicity, and enhanced overall biocompatibility [77, 79]. Antibacterial SFB nanocomposites incorporated with *ex situ* synthesized GO [80], ZnO [81–83], TiO$_2$ [84, 85], and CaO$_2$ NPs [86, 87] have been previously developed and evaluated for diverse biomedical applications such as wound healing, bone regeneration, and urethral tissue engineering (Table 2). Dhas et al. fabricated AgNPs impregnated B. mori silk fibers using two different *in situ* and *ex situ* approaches [77]. The results of their study demonstrated that *in situ* prepared fibers had larger ZOI and a higher reduction efficiency after 24 h against both *S. aureus* and *P. aeruginosa* bacteria compared to *ex situ* fabricated fibers.

Despite their versatile biomedical applications and broad-spectrum antibacterial activity, the inorganic nanomaterials/SFBs composites have not yet found their way into clinical practice due to the unforeseen risks associated with their safety and stability in long-term use. Owing to their small size, nanoparticles can cross biological barriers, penetrate tissues, and interact with cells and intracellular organelles leading to membrane disintegration, DNA modification, mitochondrial apoptosis, and cell death. In addition, depending on their physiochemical properties such as shape, charge, and wettability nanoparticles might agglomerate and accumulate in tissues and organs inducing immune responses [88, 89]. Therefore, further research is essential to fully evaluate and identify the effect of nanoparticles size, shape, charge, and chemical composition on their toxicological properties and develop novel, green methods of synthesis to obviate the use of hazardous chemicals and enhance their biocompatibility.

3.3 Inherently antibacterial polymers and peptides

Polymers and peptides with inherent antibacterial properties have been widely used as additives for SF to develop antibacterial SFBs that can resist infection and function properly when used *in vivo* (Table 3). Owing to its biocompatibility, biodegradability, and nontoxic origins, chitosan is the most studied antibacterial polymer in combination with SF for different biomedical applications such as wound healing, development of blood contacting devices, and tissue engineering [104]. Chitosan is a linear cationic polysaccharide produced by basic deacetylation of chitin, originally extracted from the shells of crustaceans and insects. The bactericidal activity of chitosan is believed to be mainly associated with the protonation of amino groups at low pH values (<pKa≈6.5) and their consequent electrostatic interaction with negatively charged bacterial cell membranes [105]. This interaction causes damages in the bacterial cell wall, impairs vital bacterial functions, and ultimately results in cell death. At higher pH values, where chitosan has a lower charge density, other bactericidal mechanisms such as hydrophobic interactions and chelation effects predominate [106, 107]. Other polymers with inherent bactericidal activity such as polyethylenimine (PEI), polypropylene (PP), and Poly (hexamethylene biguanide) hydrochloride (PHMB) have also been combined with SF for development of antibacterial wound dressings, scaffolds, and

sutures (Table 3). Electrospun SF/PEI nanofibers were shown to have a strong inhibitory effect against gram positive *S. aureus* and gram negative *P. aeruginosa* bacteria after 5h and did not show any *in vitro* cytotoxicity against L929 fibroblast cells [108]. In a study by Gogoi et al. PP was grafted onto multifilament yarns (d=~100 μm) of a non-mulberry *Antheraea assama* silk fibroin (AASF) through a plasma graft polymerization process to develop antibacterial sutures [109]. AASF yarn was first sterilized using Ar plasma and PP was grafted onto its surface using Ar/propylene plasma discharge. The resulting AASF/PP sutures showed a ZOI of 35±0.01 mm against gram negative *E. coli* bacteria after 24 h *in vitro* and remarkably improved the wound healing process when tested *in vivo* on rabbits, with complete healing after 16 days compared to 25 days for only Ar plasma treated AASF sutures. In another study, PHMB/SF porous sponges were fabricated through electrostatic interactions and freeze-drying method and were shown to have antibacterial activity against *S. aureus* and *E. coli* bacteria at PHMB/SF ratios of higher than 2/100 when tested *in vitro* by a 24 h disc diffusion assay [110].

In addition to polymers, in the last decade, there has been an increasing interest into antimicrobial peptides (AMPs) as effective antimicrobial therapeutics. AMPs are a diverse class of small molecular weight proteins with broad spectrum antibacterial activity that constitute the first line of defense in the innate immune system of different organisms [111]. AMPs are mainly composed of cationic and hydrophilic regions and can acquire amphipathic a-helical conformations that facilitate their penetration through the phospholipid bilayer membrane of the bacteria leading to inhibition of vital biological processes and cell death [112]. In fact, the cationic nature of AMPs is attributed to the presence of positively charged amino acids such as lysine and arginine in their structure allowing them to target the negatively charged membranes of bacteria causing perforation and cell lysis as well. Due to their disrupting effects on the bacterial cell wall and alteration of membrane permeability, AMPs are good candidates to be used in conjunction with other antibacterial agents to yield a more efficacious bactericidal activity [113]. In addition to the discussed mechanisms of action, AMPs can also exert their antibacterial effect by modulating and activating the host immune system [114]. Compared to conventional antibiotic treatments, AMPs offer many advantages including higher efficacy, environmental friendliness, and lower possibility of developing bacterial resistance due to their mainly physiomechanical membrane-targeted mechanism of action [115]. In addition, given the neutral zwitterionic composition of eukaryotic cell membranes, AMPs demonstrate minimized mammalian cell toxicity and a highly selective bactericidal activity [116].

There have been several efforts to fabricate antibacterial SFBs using both naturally occurring and synthetic AMPs (Table 3). Physical fabrication methods reported so far include dip-coating of SF sutures in AMP solution [117] and electrospinning of SF/AMP solutions [118] for development of antibacterial nanofibrous wound dressings. However, to overcome the rapid leaching of the antimicrobial agent associated with the physical methods of synthesis, chemical conjugation approaches have been proposed. Covalent attachment of AMPs to SFBs has been mainly carried out through carbodiimide chemistry. The chemical grafting of AMPs such as cecropin B [119], Cys-KR12 [120], and L-Cysteine [121] onto different SF substrates via EDC-NHS coupling have been reported for fabrication of antibacterial wound

dressings and implantable biomaterials that have shown strong antibacterial activity toward both gram positive and gram negative bacteria and had no demonstrated cytotoxicity (further details can be found in Table 3). Other chemical methods such as enzymatic oxidation of SF with tyrosinase and consequent grafting of ɛ-polylysine has also been demonstrated by Wang et al with about ~1.97 log reduction in *S. aureus* bacteria after 18 h, however cytotoxicity assays were not performed to further evaluate the biocompatibility of these materials [122]. In addition to physical and chemical methods of synthesis, Gomes et al. employed a bioengineering approach in which they designed and cloned three fusion AMPs (human neutrophil defensin 2, human neutrophil defensins 4, and hepcidin) to modify the spider silk [123]. The genetically engineered spider silk demonstrated antibacterial activity against *E. coli* and *S. aureus* according to a 24 h radial diffusion assay. Nevertheless, some of the major limitations regarding the development of recombinant SF proteins include the poor yield and the challenging scale-up process [124].

Quaternary ammonium compounds (QACs) are another type of polymeric substances with potent antimicrobial properties that have been previously used to develop antibacterial silk sutures [125]. QACs are cationic surfactants with a nitrogen atom, covalently bonded to four aryl/alkyl chains. Similar to the other antimicrobial polymers and peptides, QACs act on bacteria through electrostatic interactions with the membrane. The lipophilic structure of the alkyl chains enables the QAC permeation through the bacterial membrane where it will disrupt structural proteins and enzymes leading to cell death [126]. The length of the alkyl chains as well as the charge density are determining factors in the bactericidal effectiveness of the QACs [127]. Silk sutures coated with a 25% solution of K21 quaternary ammonium compound demonstrated a long lasting ZOI against *Porphyromonas gingivalis* (*P. gingivalis*) and *Enterococcus Faecalis* (*E. faecalis*) after 12 days in culture.

While the development of antibacterial SFBs using bactericidal polymers and peptides offers great promise *in vitro*, there remains several pitfalls that need to be addressed before their clinical translation. For instance, the emergence of resistant bacteria, although slower compared to antibiotic treatments, have been reported after long term use of AMPs. There are also great concerns regarding the bacteria developing resistance toward host-defense peptides after exposure to high doses of therapeutic AMPs [128]. The mechanisms underlying the evolution of bacterial resistance toward AMPs are described in a review by Sierra et al [113]. Aside from the issues related to bacterial resistance, AMPs face other limitations as well, such as high production costs, short half-life, and lack of stability *in vivo* due to degradation by proteases [129]. In addition, the adverse long-term effects of AMPs are not yet fully known, given that they can induce immunogenicity and demonstrate hemolytic activity according to previous studies [130]. The use of delivery systems such as SFBs has been proposed as a viable solution to overcome some of the mentioned limitations associated with AMPs. However, to further enable their practical clinical applications, active research into designing new AMPs with modified properties (e. g. reduced toxicity, prolonged stability, and enhanced efficacy) and rigorous *in vivo* studies using suitable animal models are required.

3.4   Plant extracts

Plants extracts have been used for medicinal purposes [147] since ancient times and in the last decade, they have gained attention as natural antioxidants and antibacterial agents to be used in combination with polymers such as SFBs for various biomedical applications (Table 4). Thus far, herbal extracts such as olive leaf, thymol, Nigella sativa, Baicalein, Pistacia terebinthus, Pistacia lentiscus, and Hypericum empetrifolium, as well as manuka honey have been combined with SFBs mostly through electrospinning method for wound dressing applications. The antibacterial and antioxidant properties of these plant extracts are believed to be mainly attributed to the presence of abundant phenolic compounds in their structure such as phenolic acids, tannins, flavonoids, carvacrol, and thymoquinone [148, 149]. In an attempt to determine the correlation between the phenolic content and antibacterial activity, Shan. et al studied 46 different herbal extracts by measuring their total phenolic content and evaluating their bacterial inhibition efficiency [150]. They found that the bactericidal activity of an herbal extract is directly influenced by its phenolic content and plant extracts with higher levels of phenolic compounds exhibited stronger antibacterial activity.

Phenolic compounds are important secondary metabolites and a part of defense mechanisms in plants which have potent antioxidant and antibacterial activity. Depending on their type and molecular structure, plant-derived phenolics exhibit different mechanisms of antibacterial action such as interfering with integral proteins and enzymes resulting in the alteration of cytoplasmic membrane, dysfunction in the metabolic activity, impairing of the genetic material, and affecting the electron and nutrient transfer in bacterial cells [150, 151]. Additionally, many phenolic containing herbal extracts have been reported to have anti-quorum sensing and biofilm suppressing activities as well [152]. In a study by Chan et al., baicalein (BAI), a Chinese herbal extract, was blended with SF to electrospin antibacterial SF fibers for wound dressing applications. Polyvinylpyrrolidone (PVP) was added to the mixture to further control the release of BAI from the dressings. The SF/PVP/BAI mats were tested against *S. aureus* which is one of the most common bacteria found in the mucous membranes and soft tissue infections in humans and 88.2–98.9% of bacteria reduction was observed after 24 h contact with the mats. The SF/PVP/BAI mats were also able to reduce infection and improve the healing rate when tested *in vivo* in a *S. aureus* infected mouse wound model.

Due to their different modes of action compared to antibiotics, herbal phenolic compounds offer promising potential for treatment of the antibiotic resistant bacteria. However, a major setback regarding the use of plant extracts as antibacterial agents is the lack of established protocols and set criteria for evaluation of their antibacterial effect resulting in contradictory results. Moreover, the high diversity of phenolic compounds and their different antibacterial effects against various bacterial strains also add up to the complication [153]. Therefore, there is a need for more defined and standard methods of investigation to make direct comparison between the results of different studies possible.

3.5   Bioinspired approaches

Biofilm formation on the surface of indwelling medical devices and implants is a major problem leading to implant failure, significant morbidity and even mortality among the

patients. The biofilm starts to form when bacteria adhere to a surface and produce an extracellular polymeric substance which secures their attachment and growth [164]. Therefore, there have been many efforts to provide the surface of biomedical materials with antibiofouling properties. In this regard, nature provides an infinite source of inspiration for researchers and scientists to design surfaces that can repel bacteria and inhibit their colonization. Several examples of natural antibiofouling surfaces can be found in animals' skin (e.g. shark, gecko), insect wings (e.g. cicada, butterfly), and plant leaves (e.g. lotus, rice) that have evolved unique topographical and chemical features to resist bacterial contamination [165]. The presence of hierarchical micro/nanoscopic patterns on the surface of these living organisms endow them with low adhesion and superhydrophobic and self-cleaning properties. Micro/nano-patterned surfaces minimize the attachment of bacteria by offering a significantly smaller contact area and an intrinsically low surface energy. They can also kill the bacteria upon contact by physically rupturing or deforming their cell wall membrane [166].

Inspired by the intricate architecture of natural antifouling surfaces and with recent advances in micro/nano-fabrication techniques, many researchers have attempted to replicate these naturally occurring topographies with the hope of reproducing their behavior on the surface of biomedical devices and implants [167]. Considering that this field is still in its infancy, there are only a few number of studies regarding the fabrication of micro/nano patterned SFBs for antifouling biomedical applications (Table 5). In a study by Mehrjou et al., homogeneous nanocones were fabricated on the surface of SF films by oxygen plasma etching for orthopedic implant application [168]. The plasma etching process resulted in the formation of new hydroxyl bonds on the surface of the nanopatterned films therefore increasing the surface energy by around 176%. The hydrophilic nanopatterned SF films could reduce the adhesion of both Gram-negative (*E. coli*) and Gram-positive (*S. aureus*) bacteria by more than 90%, while increased the proliferation of osteoblast cells by 30%. In another study by Tullii et al. [169] nanostripes and microwells with different diameters were fabricated on the surface of SF films employing a soft lithography approach. The results of their study demonstrated that the patterned SF films were able to reduce the number of adhered *E. coli* by 66% compared to flat SF films and at the same time supported the adhesion and proliferation of mammalian cells (HEK-293).

Novel bioinspired development of antifouling micro/nano patterned surfaces provides an alternative drug-free route for prevention of biomaterials associated infections. In contrary to the conventional chemistry-based approaches which require the continuous low-dose release of antibacterial agents leading to the emergence of resistant bacteria, the bioinspired micro/nano scale surface topographies promise a long-term solution, killing the bacteria through a mechanical mechanism [170]. However, this also poses a limitation on the use of micro/nano-patterned surfaces for antibacterial purposes as the bactericidal effect is only achieved if the bacteria come into direct contact with the surface. Moreover, there are concerns regarding the mechanical stability of these patterns for long-term *in vivo* applications. Physical defects in the fabricated micro/nano-structures might cause complications such as localized platelet accumulation, biofilm formation, and unwanted cytotoxic effects [171]. It is also important to note that the size, shape, spacing and type of the micro/nano-patterns as well as the type of invading bacteria dictates the bactericidal response [172]. Therefore,

finding a particular surface pattern that is effective against all types of bacteria remains a major scientific challenge. In addition to the bactericidal activity, the cytocompatibility of the micro/nano-patterns should also be considered carefully. Cytotoxic responses have been reported in the past for mico/nano scale surface structures with high aspect ratio [173]. Therefore, utmost importance must be given to investigating the stability and potential short and long-term effects of these surfaces in future studies.

In addition to surface-mediated bactericidal mechanisms, many living organisms produce antibacterial molecules as part of their defense system against pathogens. One of such natural products is nitric oxide (NO), a free-radical gas molecule with manifold physiological functions [174]. NO is produced endogenously from L-arginine by nitric oxide synthase enzymes in the 10^{-12}-10^{-6} M range. At lower nanomolar concentration (10^{-12}-10^{-9} M), NO is produced by endothelial (eNOS) and neuronal (nNOS) nitric oxide synthases to regulate vasodilation, angiogenesis, and neurotransmission and at higher micromolar concentrations (10^{-9}-10^{-6} M), it is produced by inducible nitric oxide synthase (iNOS) in macrophages as a potent antimicrobial agent to eradicate foreign pathogens [175].

NO possesses a broad-spectrum antimicrobial activity, acting upon bacteria, viruses, and fungi through multiple different mechanisms [176]. Owing to its small size and lipophilic nature, NO can easily diffuse through the bacterial cell membranes where it can cause detrimental effects on different bacterial cell components and functions. Being a free radical, NO readily reacts with oxygen and superoxides to generate reactive nitrogen and oxygen byproducts that can impose oxidative and nitrosative damage on bacterial membrane lipids, proteins, metabolic enzymes, and DNA leading to their inhibition or death [177]. The multi-mechanistic antibacterial activity of NO makes it extremely difficult for bacteria to develop resistance, therefore, offering a promising alternative to conventional antibiotics [178, 179].

In the recent years, many researchers have attempted to mimic the endogenous production of NO by developing materials that can deliver NO exogenously for different biomedical applications such as blood contacting medical devices [180–182], urinary catheters [183], endotracheal tubes [184], tissue engineering scaffolds [185, 186], and wound dressings [187, 188]. To overcome the limitations associated with direct delivery of NO including its gaseous state, high reactivity, and short half-life, various NO donor molecules (organic nitrates and nitrites, *N*-diazeniumdiolates, and *S*-nitrosothiols (RSNOs)) have been developed and incorporated into organic and inorganic substrates [189]. Incorporation of the NO donors in a substrate offers many advantages such as improving the NO release kinetics, allowing for a more sustained and tunable NO delivery, and minimizing the potential cytotoxic effects, therefore enabling the development of versatile biocompatible materials with potent antibacterial activity [190]. In addition, exogenous delivery of NO at concentrations as low as 450 pM has been shown to effectively disperse antibiotic resistant biofilms into a planktonic state by increasing the intracellular phosphodiesterase activity of the biofilm, leading to an elevated rate of cyclic di-GMP degradation, ultimately resulting in the disintegration of the biofilm [191].

Natural polymers such as SF offer an interesting platform for NO delivery due to their biocompatible degradation products, reduced immune response, large availability, and lower cost compared to synthetic delivery platforms [192]. Our group has recently demonstrated the fabrication of NO releasing SF NPs through an antisolvent/self-assembling approach [193]. *S*-Nitroso-*N*-acetylpenicillamine (SNAP), a synthetic tertiary RSNO, was loaded into SF NPs by adding SNAP/ethanol solution to an aqueous SF solution and freeze-thawing the mixture. The prepared SNAP-SF NPs could release a total of $1.31 \pm 0.02 \times 10^{-10}$ mol mg^{-1} NO over a 24 h period and showed a concentration-dependent antibacterial activity against methicillin-resistant *Staphylococcus aureus* (MRSA) and *E. coli*, inhibiting more than 99.9% of the bacteria at a concentration of 10 mg/mL. This study was the first to demonstrate the implementation of NO as an antibacterial additive for SF and therefore can open up new avenues for more exploration in this area and development of novel NO releasing antibacterial SFBs in the future.

3.6   Combination approaches

The multi-drug resistant bacteria, emerged by the widespread use of antibiotics and other antimicrobial agents, pose a severe threat to public health worldwide. One effective approach to combat this type of bacteria is the combinational use of different antibacterial agents [195]. Combination therapies using antibacterial agents with multiple targets of action can reduce the chances of development of resistance, decrease the use of excess drug doses and occurrence of adverse side effects, and often results in synergistically higher antibacterial activity [196].

Thus far, development of antibacterial SFBs using chitosan along with other antibacterial agents such as penicillin [197], ZnO nanoparticles [198], and water crude longan seed extract [199] have been reported in the literature. These studies are all in agreement that a higher bactericidal efficacy can be obtained by using a combination of chitosan with another antibacterial agent as additives for SFBs (Table 6). Moreover, in a study by Zhou et al. Ag NPs in combination with gentamicin were used to fabricate antibacterial SF based coatings for Ti implants [200]. The results of the study showed a significantly higher bactericidal activity by synergistic combination of gentamicin and Ag NPs at concentrations far below their minimum inhibitory concentration. The prepared coatings were able to reduce the bacterial adhesion on the surface of Ti implants by 95%. In another study by Vieira et al. Ag NPs were reduced by SF in a basic condition to make conductive SF/Ag NPs gels [201]. By applying an electric current to the gels, 50% higher ROS generation were obtained compared to control. The SF gels made with 50% AgNO$_3$ had a conductivity of 1.5 S cm^{-1} and were able to inhibit 80% of *E. coli* in 1 min with electric current being applied. The fabrication of electrospun SF based nanofibers containing a combination of *S*-Nitrosoglutathione (GSNO) NO donor molecules and type I collagen peptides (CP) has also been reported as an antibacterial wound dressing for treatment of ischemic chronic wounds [202]. According to a 24 h disk diffusion assay the fibers containing CP alone showed only moderate antibacterial activity against *E. coli* and *P.* aeruginosa and low activity against *S. aureus*, while addition of GSNO significantly increased the corresponding zones of inhibition and antibacterial activity against these bacteria.

Overall, the combination approaches offer an interesting alternative to inefficient monotherapy methods and can reduce the risks associated with the emergence of antibacterial resistance. With a multitude of antibacterial agents available and different material formats that SF can acquire, there is an opportunity to design a plethora of novel antibacterial SFBs. However, the exact molecular mechanisms of all antibacterial components and their cross interactions should be carefully considered before fabrication to obtain a highly synergistic bactericidal efficiency and prevent any undesired side effects, respectively.

4. Antibacterial SFBs in clinical trial

As an FDA approved material, SF has been the subject of considerable interest for development of cosmetics, biomedical products, and clothing. Many of these products such as silk masks, gels, sutures, wound dressings (Fibroheal™ Ag), tissue scaffolds (FibroFix™, SilkVoice®), and textiles (DermaSilk®) have already been commercialized and can be found on the market while several others are awaiting to pass clinical trials [206, 207]. The review paper by Holland et al. on biomedical uses of SF, presents a detailed overview of the previously passed and currently ongoing clinical trials of silk-based biomedical materials [208]. Owing to their low inflammatory responses, flexibility, oxygen permeability, tunable degradation, and good mechanical properties, SFBs are majorly used as scaffolds for tissue engineering and wound healing applications. Several examples of SF-based scaffolds, wound dressings, and surgical meshes (HQ® Matrix Soft Tissue Mesh) exist that their safety and efficacy have been tested through clinical trials and are soon to be commercially available [207]. In a recent study, a bi-layered wound dressing was fabricated by mixing SF, gelatin and sericin solutions and casting them on a silk fabric. The top-layer was crosslinked using glutaraldehyde and after several washing with glycine and deionized water, it was freeze-dried and gamma-sterilized. The final product was compared to the commercial Bactigras and showed satisfactory results in preclinical and the randomized clinical trials for safe and effective full-thickness skin wound healing [209]. The results of the preclinical evaluation of a three-layered SF-based nerve conduit (SilkBridge™), developed by an electrospinning method, was published recently [210]. When tested in a model of rat median nerve injury, the SilkBridge™ conduit demonstrated great ability to repair the function and recover the morphology of the median nerve similar to the results obtained by the reference autograft nerve reconstruction method. The SilkBridge™ nerve conduits are currently undergoing clinical studies to evaluate their safety and efficacy for the healing of digital nerve defects in humans (ClinicalTrials.gov identifier: NCT03673449). With the increasing number of SFBs becoming clinically available, combination of antibacterial agents into these materials can be a great strategy to further improve their abilities and broaden their range of applications. Despite a large body of research regarding antibacterial SFBs in the recent years and their promising applications, these materials have scarcely found their way into clinical applications. However, due to the rapidly growing nature of this field and the myriad of potential applications of antibacterial SFBs, their emergence in clinical settings is highly anticipated in the years to come.

5. Conclusions and future trends

Silk fibroin (SF) is a natural polymer that has been dominantly used for different biomedical applications owing to its unique combination of properties including super biocompatibility, excellent mechanical properties, controllable biodegradation, and versatile material formats. Many SF-based biomaterials (SFBs) have been developed so far that are used as tissue engineering scaffolds, wound dressings, sutures, and medical device coatings. Regarding the lack of inherent antibacterial activity of SF and with bacterial infection being the principal cause of biomaterials failure, there have been many attempts to endow SFBs with antibacterial properties and span their range of application. The water-based processing of SF, along with the presence of multiple functional groups (e.g. hydroxyl, carboxylic acid, and amine) in its structure have enabled the physical loading or chemical functionalization of SFBs with different antibacterial agents such as antibiotics, antibacterial polymers/ peptides, and phenolic plant extracts. In addition, the electron donating ability of SF at basic pH has made it a potent reducing and stabilizing agents for green synthesis of several bactericidal inorganic nanoparticles such as Ag NPs and Au NPs, facilitating the fabrication of antibacterial SF-based nanocomposites. However, despite a large body of studies in this area, development of bacterial resistance, low stability, high cost, and potential cytotoxic effects mark some of the major limitations associated with the use of these antibacterial agents.

Recently, increasing interest have been directed toward designing bactericidal surface patterns on SF substrates inspired by natural surfaces such as insect wings, animals' skin, and plant leaves, that can repel or kill the bacteria upon contact. These bioinspired approaches advantageously eliminate the use of toxic chemicals and have proved effective in reducing the surface fouling and mitigating bacterial infections. Although promising, this field is still in the early stage of its growth and further studies are required to assess the long-term efficacy of these patterns *in vivo* and find an optimized range of design parameters for maximal bactericidal action and minimal cytotoxic effects. Another recently emerging bioinspired technique to provide SFBs with antibacterial activity is the use of nitric oxide donor molecules. NO donors have been previously incorporated into various synthetic polymers for development of antibacterial medical devices and coatings and have recently found their way into natural polymers as well. Due to the versatile physiological roles of NO beside its antibacterial action, this method is highly promising for development of antibacterial SF-based platforms with therapeutic activity for different biomedical applications.

Considering the different bactericidal mechanisms offered by various methods, one powerful approach is to use a combination of these methods to design SFBs with strong synergistic bactericidal activity. However, most approaches lack adequate characterization information with unknown long-term effects and are not yet ready for clinical translation. Therefore, thorough *in vivo* studies, establishment of standard verification test protocols and criteria, and full understanding of the bactericidal mechanisms of each approach are areas that need to be worked on in future.

Acknowledgements

References

1. Mehrotra S, et al., Comprehensive review on silk at nanoscale for regenerative medicine and allied applications 2019. 5(5): p. 2054–2078.

2. Qi Y, et al., A review of structure construction of silk fibroin biomaterials from single structures to multi-level structures 2017. 18(3): p. 237.

3. Tomeh MA, Hadianamrei R, and Zhao XJP, Silk fibroin as a functional biomaterial for drug and gene delivery 2019. 11(10): p. 494.

4. Kasoju N and Bora U.J.A.h.m., Silk fibroin in tissue engineering 2012. 1(4): p. 393–412.

5. Fan S, et al., Silk materials for medical, electronic and optical applications 2019. 62(6): p. 903–918.

6. Janani G, et al., Insight into silk-based biomaterials: From physicochemical attributes to recent biomedical applications 2019. 2(12): p. 5460–5491.

7. Gomes S, et al. , Biological responses to spider silk-antibiotic fusion protein. J Tissue Eng Regen Med, 2012. 6(5): p. 356–68. [PubMed: 22514077]

8. Jao D, Mou X, and Hu X, Tissue Regeneration: A Silk Road. J Funct Biomater, 2016. 7(3).

9. Chouhan D and Mandal B.B.J.A.b., Silk biomaterials in wound healing and skin regeneration therapeutics: From bench to bedside 2020. 103: p. 24–51.

10. Nguyen TP, et al., Silk fibroin-based biomaterials for biomedical applications: a review 2019. 11(12): p. 1933.

11. Kundu SC, et al., Natural protective glue protein, sericin bioengineered by silkworms: potential for biomedical and biotechnological applications 2008. 33(10): p. 998–1012.

12. Abdel-Fattah WI, Atwa N, and Ali G.W.J.P.i.b., Influence of the protocol of fibroin extraction on the antibiotic activities of the constructed composites 2015. 4(2): p. 77–88.

13. Rockwood DN, et al., Materials fabrication from Bombyx mori silk fibroin 2011. 6(10): p. 1612.

14. Arami M, et al., Degumming of Persian silk with mixed proteolytic enzymes 2007. 106(1): p. 267–275.

15. Freddi G, Mossotti R, and Innocenti R.J.J.o.B., Degumming of silk fabric with several proteases 2003. 106(1): p. 101–112.

16. Khan MMR, et al., Physical properties and dyeability of silk fibers degummed with citric acid 2010. 101(21): p. 8439–8445.

17. Long J-J, et al., Application of low-pressure plasma pretreatment in silk fabric degumming process 2008. 28(6): p. 701–713.

18. Li G, et al., Surface modification and functionalization of silk fibroin fibers/fabric toward high performance applications 2012. 32(4): p. 627–636.

19. Inoue S, et al. , Silk Fibroin of Bombyx mori Is Secreted, Assembling a High Molecular Mass Elementary Unit Consisting of H-chain, L-chain, and P25, with a 6:6:1 Molar Ratio*. Journal of Biological Chemistry, 2000. 275(51): p. 40517–40528.

20. Koh L-D, et al., Structures, mechanical properties and applications of silk fibroin materials 2015. 46: p. 86–110.

21. Pandey V, et al., Silk as a leading-edge biological macromolecule for improved drug delivery 2020. 55: p. 101294.

22. Ghalei S, et al. , Enhanced cellular response elicited by addition of amniotic fluid to alginate hydrogel-electrospun silk fibroin fibers for potential wound dressing application. Colloids and Surfaces B: Biointerfaces, 2018. 172: p. 82–89. [PubMed: 30138790]

23. Ribeiro VP, et al., Silk fibroin-based hydrogels and scaffolds for osteochondral repair and regeneration 2018: p. 305–325.

24. Farokhi M, et al., Functionalized silk fibroin nanofibers as drug carriers: Advantages and challenges 2020. 321: p. 324–347.

25. You R, et al., Regenerated egg white/silk fibroin composite films for biomedical applications 2017. 79: p. 430–435.

26. Gianak O, et al., A review for the synthesis of silk fibroin nanoparticles with different techniques and their ability to be used for drug delivery 2019. 15(4): p. 339–348.

27. Montalbán MG, et al., Production of curcumin-loaded silk fibroin nanoparticles for cancer therapy 2018. 8(2): p. 126.

28. Mao B, et al., Cyclic cRGDfk peptide and Chlorin e6 functionalized silk fibroin nanoparticles for targeted drug delivery and photodynamic therapy 2018. 161: p. 306–320.

29. Rahmani H, et al., Preparation and characterization of silk fibroin nanoparticles as a potential drug delivery system for 5-fluorouracil 2019. 9(4): p. 601.

30. Francolini I, et al., Antifouling and antimicrobial biomaterials: an overview 2017. 125(4): p. 392–417.

31. Reichman DE and Greenberg JA, Reducing surgical site infections: a review. Reviews in obstetrics & gynecology, 2009. 2(4): p. 212–221. [PubMed: 20111657]

32. Ahmed W, Zhai Z, and Gao CJMTB, Adaptive antibacterial biomaterial surfaces and their applications 2019. 2: p. 100017.

33. Greenhalgh R, et al., Antimicrobial strategies to reduce polymer biomaterial infections and their economic implications and considerations 2019. 136: p. 1–14.

34. Kaushik S, et al., Silk Fibroin: An Emerging Biocompatible Material for Application of Enzymes and Whole Cells in Bioelectronics and Bioanalytical Sciences 2020. 6(8): p. 4337–4355.

35. Seves A, et al., The microbial degradation of silk: a laboratory investigation 1998. 42(4): p. 203–211.

36. Tabei Y, et al., Application of insoluble fibroin film as conditioning film for biofilm formation 2011. 23(4): p. 195–205.

37. Kaushik S, et al., Thin films of silk fibroin and its blend with chitosan strongly promote biofilm growth of Synechococcus sp. BDU 140432 2016. 479: p. 251–259.

38. Bidossi A, et al., In Vitro Evaluation of Gentamicin or Vancomycin Containing Bone Graft Substitute in the Prevention of Orthopedic Implant-Related Infections 2020. 21(23): p. 9250.

39. Nair MB, et al. , Infection and tissue engineering in segmental bone defects--a mini review. Curr Opin Biotechnol, 2011. 22(5): p. 721–5. [PubMed: 21354782]

40. Kohanski MA, Dwyer DJ, and Collins JJ, How antibiotics kill bacteria: from targets to networks. Nature Reviews Microbiology, 2010. 8(6): p. 423–435. [PubMed: 20440275]

41. Lan Y, et al., Preparation and characterisation of vancomycin-impregnated gelatin microspheres/ silk fibroin scaffold 2014. 25(1): p. 75–87.

42. Campoccia D, et al. , Antibiotic-loaded biomaterials and the risks for the spread of antibiotic resistance following their prophylactic and therapeutic clinical use. Biomaterials, 2010. 31(25): p. 6363–77. [PubMed: 20542556]

43. Steinstraesser L, et al., Colistin-loaded silk membranes against wound infection with Pseudomonas aeruginosa 2011. 127(5): p. 1838–1846.

44. Srivastava CM, et al., Dextrose modified flexible tasar and muga fibroin films for wound healing applications 2017. 75: p. 104–114.

45. Song J, et al., Electrospun nanofibrous silk fibroin membranes containing gelatin nanospheres for controlled delivery of biomolecules 2017. 6(14): p. 1700014.

46. Hassani Besheli N, et al., Sustainable release of vancomycin from silk fibroin nanoparticles for treating severe bone infection in rat tibia osteomyelitis model 2017. 9(6): p. 5128–5138.

47. Lan Y, et al., Therapeutic efficacy of antibiotic-loaded gelatin microsphere/silk fibroin scaffolds in infected full-thickness burns 2014. 10(7): p. 3167–3176.

48. Ojah N, et al., Chitosan coated silk fibroin surface modified by atmospheric dielectric-barrier discharge (DBD) plasma: a mechanically robust drug release system 2019. 30(13): p. 1142–1160.

49. Choudhury AJ, et al., Controlled antibiotic-releasing Antheraea assama silk fibroin suture for infection prevention and fast wound healing 2016. 159(2): p. 539–547.

50. Han C, et al., Electrophoretic deposition of gentamicin-loaded silk fibroin coatings on 3D-printed porous cobalt–chromium–molybdenum bone substitutes to prevent orthopedic implant infections 2017. 18(11): p. 3776–3787.

51. Zhang Z, et al., Electrophoretic deposition of tetracycline modified silk fibroin coatings for functionalization of titanium surfaces 2014. 303: p. 255–262.

52. Arpaçay P and Türkan UJBEBT, Development of antibiotic-loaded silk fibroin/hyaluronic acid polyelectrolyte film coated CoCrMo alloy 2016. 61(5): p. 463–474.

53. Wu M, et al., Silk microfibrous mats with long-lasting antimicrobial function 2020.

54. Khatoon Z, et al., Bacterial biofilm formation on implantable devices and approaches to its treatment and prevention 2018. 4(12): p. e01067.

55. Gebreyohannes G, et al., Challenges of intervention, treatment, and antibiotic resistance of biofilm-forming microorganisms 2019. 5(8): p. e02192.

56. Bradner SA, et al., Silk Protein Bioresorbable, Drug- Eluting Ear Tubes: Proof- of- Concept 2019. 8(3): p. 1801409.

57. Sharma S, et al., Silk fibroin nanoparticles support in vitro sustained antibiotic release and osteogenesis on titanium surface 2016. 12(5): p. 1193–1204.

58. Shi C, et al., An antibacterial and absorbable silk-based fixation material with impressive mechanical properties and biocompatibility 2016. 6: p. 37418.

59. Ahadi F, Khorshidi S, and Karkhaneh AJEPJ, A hydrogel/fiber scaffold based on silk fibroin/ oxidized pectin with sustainable release of vancomycin hydrochloride 2019. 118: p. 265–274.

60. Dizaj SM, et al., Antimicrobial activity of the metals and metal oxide nanoparticles 2014. 44: p. 278–284.

61. Slavin YN, et al., Metal nanoparticles: understanding the mechanisms behind antibacterial activity 2017. 15(1): p. 1–20.

62. Abo- zeid Y, Williams GRJWIRN, and Nanobiotechnology, The potential anti- infective applications of metal oxide nanoparticles: A systematic review 2020. 12(2): p. e1592.

63. Augustine R, Hasan A.J.J.o.D.D.S., and Technology, Emerging applications of biocompatible phytosynthesized metal/metal oxide nanoparticles in healthcare 2020. 56: p. 101516.

64. Das S and Dhar BBJRA, Green synthesis of noble metal nanoparticles using cysteine-modified silk fibroin: catalysis and antibacterial activity 2014. 4(86): p. 46285–46292.

65. Schnaider L, et al., Biocompatible Hybrid Organic/Inorganic Microhydrogels Promote Bacterial Adherence and Eradication in Vitro and in Vivo 2020. 20(3): p. 1590–1597.

66. Fei X, et al., Green synthesis of silk fibroin-silver nanoparticle composites with effective antibacterial and biofilm-disrupting properties 2013. 14(12): p. 4483–4488.

67. Li G, et al., Preparation of antibacterial degummed silk fiber/nano-hydroxyapatite/polylactic acid composite scaffold by degummed silk fiber loaded silver nanoparticles 2019. 30(29): p. 295101.

68. Ribeiro M, et al., Antibacterial silk fibroin/nanohydroxyapatite hydrogels with silver and gold nanoparticles for bone regeneration 2017. 13(1): p. 231–239.

69. Rao BL, et al., Rapid synthesis of gold nanoparticles using silk fibroin: Characterization, antibacterial activity, and anticancer properties 2017. 50(4): p. 289–297.

70. Abbasi AR, Akhbari K, and Morsali A.J.U.s., Dense coating of surface mounted CuBTC metal– organic framework nanostructures on silk fibers, prepared by layer-by-layer method under ultrasound irradiation with antibacterial activity 2012. 19(4): p. 846–852.

71. Murphy AR, John PS, and Kaplan DL, Modification of silk fibroin using diazonium coupling chemistry and the effects on hMSC proliferation and differentiation. Biomaterials, 2008. 29(19): p. 2829–2838. [PubMed: 18417206]

72. Selvakannan P, et al., Synthesis of aqueous Au core– Ag shell nanoparticles using tyrosine as a pH-dependent reducing agent and assembling phase-transferred silver nanoparticles at the air–water interface 2004. 20(18): p. 7825–7836.

73. El-Seedi HR, et al., Metal nanoparticles fabricated by green chemistry using natural extracts: biosynthesis, mechanisms, and applications 2019. 9(42): p. 24539–24559.

74. Kharlampieva E, et al., Redox-active ultrathin template of silk fibroin: effect of secondary structure on gold nanoparticle reduction 2009. 21(13): p. 2696–2704.

75. Grant AM, et al., Silk fibroin–substrate interactions at heterogeneous nanocomposite interfaces 2016. 26(35): p. 6380–6392.

76. Huang X-W, et al., Silk fibroin-assisted exfoliation and functionalization of transition metal dichalcogenide nanosheets for antibacterial wound dressings 2017. 9(44): p. 17193–17198.

77. Dhas SP, et al., Biobased silver nanocolloid coating on silk fibers for prevention of post-surgical wound infections 2015. 10(Suppl 1): p. 159.

78. Srivastava CM, Purwar R, and Gupta A.P.J.I.j.o.b.m., Enhanced potential of biomimetic, silver nanoparticles functionalized Antheraea mylitta (tasar) silk fibroin nanofibrous mats for skin tissue engineering 2019. 130: p. 437–453.

79. Belda Marín C, et al., Silk Polymers and Nanoparticles: A Powerful Combination for the Design of Versatile Biomaterials 2020. 8(1141).

80. Wang S-D, et al., Improving antibacterial activity and biocompatibility of bioinspired electrospinning silk fibroin nanofibers modified by graphene oxide 2018. 3(1): p. 406–413.

81. Cao F, et al., Porous ZnO modified silk sutures with dual light defined antibacterial, healing promotion and controlled self-degradation capabilities 2020. 8(1): p. 250–255.

82. Hadisi Z, et al., Hyaluronic Acid (HA)- Based Silk Fibroin/Zinc Oxide Core–Shell Electrospun Dressing for Burn Wound Management 2020. 20(4): p. 1900328.

83. Shubha P, et al., Ex-situ fabrication of ZnO nanoparticles coated silk fiber for surgical applications 2019. 231: p. 21–26.

84. Mehrabani MG, et al., Chitin/silk fibroin/TiO_2 bio-nanocomposite as a biocompatible wound dressing bandage with strong antimicrobial activity. 2018. 116: p. 966–976.

85. Xia Y, et al., Preparation and properties of nanometer titanium dioxide/silk fibroin blend membrane 2009. 90(2): p. 653–658.

86. Tian W, et al., Evaluation of the biomedical properties of a Ca+-conjugated silk fibroin porous material 2019. 104: p. 110003.

87. Lv X, et al., Structural and functional evaluation of oxygenating keratin/silk fibroin scaffold and initial assessment of their potential for urethral tissue engineering 2016. 84: p. 99–110.

88. Attarilar S, et al., The Toxicity Phenomenon and the Related Occurrence in Metal and Metal Oxide Nanoparticles: A Brief Review From the Biomedical Perspective 2020. 8(822).

89. Makvandi P, et al., Metal- based nanomaterials in biomedical applications: Antimicrobial activity and cytotoxicity aspects 2020. 30(22): p. 1910021.

90. Babu PJ, et al., Silver oxide nanoparticles embedded silk fibroin spuns: Microwave mediated preparation, characterization and their synergistic wound healing and anti-bacterial activity 2018. 513: p. 62–71.

91. Li P, et al., A resilient and flexible chitosan/silk cryogel incorporated Ag/Sr co-doped nanoscale hydroxyapatite for osteoinductivity and antibacterial properties 2018. 6(45): p. 7427–7438.

92. Wang B, et al., Surface modification of titanium implants by silk fibroin/Ag co-functionalized strontium titanate nanotubes for inhibition of bacterial-associated infection and enhancement of in vivo osseointegration 2021. 405: p. 126700.

93. Patil S, Singh NJC, and Biointerfaces SB, Antibacterial silk fibroin scaffolds with green synthesized silver nanoparticles for osteoblast proliferation and human mesenchymal stem cell differentiation 2019. 176: p. 150–155.

94. Patil S, et al., Green synthesized nanosilver loaded silk fibroin gel for enhanced wound healing 2015. 30: p. 30–36.

95. Pei Z, et al., Preparation and characterization of silver nanoparticles on silk fibroin/ carboxymethylchitosan composite sponge as anti-bacterial wound dressing 2015. 26(s1): p. S111– S118.

96. Jia M, et al., Efficacy of silk fibroin–nano silver against Staphylococcus aureus biofilms in a rabbit model of sinusitis 2017. 12: p. 2933.

97. Calamak S, et al., Ag/silk fibroin nanofibers: effect of fibroin morphology on Ag+ release and antibacterial activity 2015. 67: p. 99–112.

Author Manuscript

Author Manuscript

Author Manuscript

Author Manuscript

98. De Simone S, et al., Development of silver nano-coatings on silk sutures as a novel approach against surgical infections 2014. 25(9): p. 2205–2214.

99. Wang X, et al., Ag@ AgCl nanoparticles in-situ deposited cellulose acetate/silk fibroin composite film for photocatalytic and antibacterial applications 2020. 27(13): p. 7721–7737.

100. Zhu G, et al., Composite Film with Antibacterial Gold Nanoparticles and Silk Fibroin for Treating Multidrug-Resistant E. coli-Infected Wounds 2020.

101. Zhang C, et al., Silk fibroin/reduced graphene oxide composite mats with enhanced mechanical properties and conductivity for tissue engineering 2021. 197: p. 111444.

102. Zhang C, et al. , Reduced graphene oxide/titanium dioxide hybrid nanofiller-reinforced electrospun silk fibroin scaffolds for tissue engineering. Materials Letters, 2021. 291: p. 129563.

103. Eivazzadeh-Keihan R, et al. , Alginate hydrogel-polyvinyl alcohol/silk fibroin/magnesium hydroxide nanorods: A novel scaffold with biological and antibacterial activity and improved mechanical properties. International Journal of Biological Macromolecules, 2020. 162: p. 1959–1971. [PubMed: 32814101]

104. Eivazzadeh-Keihan R, et al. , Chitosan hydrogel/silk fibroin/Mg(OH)2 nanobiocomposite as a novel scaffold with antimicrobial activity and improved mechanical properties. Scientific Reports, 2021. 11(1): p. 650. [PubMed: 33436831]

105. Huang KS, et al. , Recent Advances in Antimicrobial Polymers: A Mini-Review. Int J Mol Sci, 2016. 17(9).

106. Jain A, et al., Antimicrobial polymers 2014. 3(12): p. 1969–1985.

107. Raafat D, et al., Insights into the mode of action of chitosan as an antibacterial compound 2008. 74(12): p. 3764–3773.

108. Çalamak S, et al., Silk fibroin based antibacterial bionanotextiles as wound dressing materials 2014. 43: p. 11–20.

109. Gogoi D, et al., Development of advanced antimicrobial and sterilized plasma polypropylene grafted muga (antheraea assama) silk as suture biomaterial 2014. 101(4): p. 355–365.

110. Liang A, et al., Porous Poly (Hexamethylene Biguanide) Hydrochloride Loaded Silk Fibroin Sponges with Antibacterial Function 2020. 13(2): p. 285.

111. Lei J, et al., The antimicrobial peptides and their potential clinical applications 2019. 11(7): p. 3919.

112. Kumar P, Kizhakkedathu JN, and Straus SKJB, Antimicrobial peptides: diversity, mechanism of action and strategies to improve the activity and biocompatibility in vivo 2018. 8(1): p. 4.

113. Sierra JM, et al., An overview of antimicrobial peptides and the latest advances in their development 2017. 17(6): p. 663–676.

114. Nikola S, Janine S, and Joerg O, Potential Application of Antimicrobial Peptides in the Treatment of Bacterial Biofilm Infections. Current Pharmaceutical Design, 2015. 21(1): p. 67–84. [PubMed: 25189860]

115. Magana M, et al., The value of antimicrobial peptides in the age of resistance 2020.

116. Konai MM, et al., Recent progress in polymer research to tackle infections and antimicrobial resistance 2018. 19(6): p. 1888–1917.

117. Franco AR, et al., Antimicrobial coating of spider silk to prevent bacterial attachment on silk surgical sutures 2019. 99: p. 236–246.

118. Zhang D, et al., Helicobacter pylori ribosomal protein-A2 peptide/silk fibroin nanofibrous composites as potential wound dressing 2019. 15(3): p. 507–517.

119. Bai L, et al., Surface modification and properties of Bombyx mori silk fibroin films by antimicrobial peptide 2008. 254(10): p. 2988–2995.

120. Song DW, et al., Multi-biofunction of antimicrobial peptide-immobilized silk fibroin nanofiber membrane: Implications for wound healing 2016. 39: p. 146–155.

121. Nogueira F, et al., Antimicrobial and antioxidant surface modification toward a new silk-fibroin (SF)-L-Cysteine material for skin disease management 2016. 364: p. 552–559.

122. Wang P, et al., Preparation of antibacterial silk fibroin membranes via tyrosinase- catalyzed coupling of ɛ- polylysine 2016. 63(2): p. 163–169.

123. Gomes SC, et al., Antimicrobial functionalized genetically engineered spider silk 2011. 32(18): p. 4255–4266.

124. Deptuch T and Dams-Kozlowska H, Silk Materials Functionalized via Genetic Engineering for Biomedical Applications. Materials (Basel, Switzerland), 2017. 10(12): p. 1417.

125. Meghil MM, et al., Novel coating of surgical suture confers antimicrobial activity against Porphyromonas gingivalis and Enterococcus faecalis 2015. 86(6): p. 788–794.

126. Jennings MC, Minbiole KP, and Wuest W.M.J.A.i.d., Quaternary ammonium compounds: an antimicrobial mainstay and platform for innovation to address bacterial resistance 2015. 1(7): p. 288–303.

127. Li F, Weir MD, and Xu HHK, Effects of quaternary ammonium chain length on antibacterial bonding agents. Journal of dental research, 2013. 92(10): p. 932–938. [PubMed: 23958761]

128. Moravej H, et al., Antimicrobial peptides: features, action, and their resistance mechanisms in bacteria 2018. 24(6): p. 747–767.

129. Bechinger B and Gorr S.-U.J.J.o.d.r., Antimicrobial peptides: mechanisms of action and resistance 2017. 96(3): p. 254–260.

130. Oddo A and Hansen PR, Hemolytic activity of antimicrobial peptides, in Antimicrobial Peptides 2017, Springer. p. 427–435.

131. Tu H, et al., Layer-by-layer immobilization of amphoteric carboxymethyl chitosan onto biocompatible silk fibroin nanofibrous mats 2019. 210: p. 9–16.

132. Adali T, Kalkan R, and Karimizarandi L.J.I.j.o.b.m., The chondrocyte cell proliferation of a chitosan/silk fibroin/egg shell membrane hydrogels 2019. 124: p. 541–547.

133. Xia L, et al., LBL deposition of chitosan and silk fibroin on nanofibers for improving physical and biological performance of patches 2019. 130: p. 348–356.

134. Wang J, et al., Dual-functional composite with anticoagulant and antibacterial properties based on heparinized silk fibroin and chitosan 2011. 85(2): p. 241–247.

135. Shao J, et al., Improved accumulation of TGF-β by photopolymerized chitosan/silk protein bio-hydrogel matrix to improve differentiations of mesenchymal stem cells in articular cartilage tissue regeneration 2020. 203: p. 111744.

136. Li L, et al., LBL deposition of chitosan/heparin bilayers for improving biological ability and reducing infection of nanofibers 2020.

137. Cai Z. x., et al., Fabrication of chitosan/silk fibroin composite nanofibers for wound-dressing applications 2010. 11(9): p. 3529–3539.

138. Bhardwaj N and Kundu SCJCP, Silk fibroin protein and chitosan polyelectrolyte complex porous scaffolds for tissue engineering applications 2011. 85(2): p. 325–333.

139. Chen J, et al., Enhanced physical and biological properties of silk fibroin nanofibers by layer-by-layer deposition of chitosan and rectorite 2018. 523: p. 208–216.

140. Ma X, et al., Chitosan/polydopamine layer by layer self-assembled silk fibroin nanofibers for biomedical applications 2021. 251: p. 117058.

141. Han L, et al., Mussel-inspired cryogels for promoting wound regeneration through photobiostimulation, modulating inflammatory responses and suppressing bacterial invasion 2019. 11(34): p. 15846–15861.

142. Gokila S, et al., Development of 3D scaffolds using nanochitosan/silk-fibroin/hyaluronic acid biomaterials for tissue engineering applications 2018. 120: p. 876–885.

143. Zhou Q, et al., Preparation of a multifunctional fibroin-based biomaterial via laccase-assisted grafting of chitooligosaccharide 2018. 113: p. 1062–1072.

144. Hu W, et al., High Flexible and Broad Antibacterial Nanodressing Induces Complete Skin Repair with Angiogenic and Follicle Regeneration 2020: p. 2000035.

145. Karatepe UY and Ozdemir TJBM, Improving mechanical and antibacterial properties of PMMA via polyblend electrospinning with silk fibroin and polyethyleneimine towards dental applications 2020. 5(3): p. 510–515.

146. Wang R, et al., Forward Wound Closure with Regenerated Silk Fibroin and Polylysine-Modified Chitosan Composite Bioadhesives as Dressings 2020. 3(11): p. 7941–7951.

147. Bereksi MS, et al., Evaluation of antibacterial activity of some medicinal plants extracts commonly used in Algerian traditional medicine against some pathogenic bacteria 2018. 10(3).

148. Tungmunnithum D, et al., Flavonoids and Other Phenolic Compounds from Medicinal Plants for Pharmaceutical and Medical Aspects: An Overview 2018. 5(3): p. 93.

149. Asadi H, et al. , A multifunctional polymeric coating incorporating lawsone with corrosion resistance and antibacterial activity for biomedical Mg alloys. Progress in Organic Coatings, 2021. 153: p. 106157.

150. Shan B, et al. , The in vitro antibacterial activity of dietary spice and medicinal herb extracts. Int J Food Microbiol, 2007. 117(1): p. 112–9. [PubMed: 17449125]

151. Escobar A, et al. , Thymol bioactivity: A review focusing on practical applications. Arabian Journal of Chemistry, 2020. 13(12): p. 9243–9269.

152. Takó M, et al. , Plant Phenolics and Phenolic-Enriched Extracts as Antimicrobial Agents against Food-Contaminating Microorganisms. Antioxidants (Basel, Switzerland), 2020. 9(2): p. 165.

153. Ríos JL and Recio MC, Medicinal plants and antimicrobial activity. J Ethnopharmacol, 2005. 100(1–2): p. 80–4. [PubMed: 15964727]

154. Chan WP, Huang KC, and Bai M.Y.J.J.o.B.M.R.P.B.A.B., Silk fibroin protein- based nonwoven mats incorporating baicalein C hinese herbal extract: preparation, characterizations, and in vivo evaluation 2017. 105(2): p. 420–430.

155. Nourmohammadi J, et al., Physicochemical and Antibacterial Characterization of Nanofibrous Wound Dressing from Silk Fibroin-polyvinyl Alcohol-Elaeagnus Angustifolia Extract 2020. 21(3): p. 456–464.

156. Hixon KR, et al., A comparison of tissue engineering scaffolds incorporated with Manuka honey of varying UMF 2017. 2017.

157. Yang X, et al., Green electrospun Manuka honey/silk fibroin fibrous matrices as potential wound dressing 2017. 119: p. 76–84.

158. Muthumanickkam A, et al., Development of herb based (Nigella sativa) eri silk nanofibrous mat for biomedical applications 2020. 22: p. 585–588.

159. Do an G, et al., Bioactive sheath/core nanofibers containing olive leaf extract 2016. 79(1): p. 38–49.

160. Huang K, et al., PLCL/Silk fibroin based antibacterial nano wound dressing encapsulating oregano essential oil: Fabrication, characterization and biological evaluation 2020. 196: p. 111352.

161. Basal G, et al., Antibacterial properties of silk fibroin/chitosan blend films loaded with plant extract 2010. 11(1): p. 21–27.

162. Miguel SP, et al., Production and characterization of electrospun silk fibroin based asymmetric membranes for wound dressing applications 2019. 121: p. 524–535.

163. Zakeri-Siavashani A, et al., Three dimensional spongy fibroin scaffolds containing keratin/vanillin particles as an antibacterial skin tissue engineering scaffold 2020: p. 1–12.

164. Arciola CR, Campoccia D, and Montanaro LJNRM, Implant infections: adhesion, biofilm formation and immune evasion 2018. 16(7): p. 397–409.

165. Jaggessar A, et al., Bio-mimicking nano and micro-structured surface fabrication for antibacterial properties in medical implants 2017. 15(1): p. 1–20.

166. Maleki E, et al., Analyzing the mechano-bactericidal effect of nano-patterned surfaces on different bacteria species 2020: p. 126782.

167. Tripathy A, et al., Natural and bioinspired nanostructured bactericidal surfaces 2017. 248: p. 85–104.

168. Mehrjou B, et al., Antibacterial and cytocompatible nanoengineered silk-based materials for orthopedic implants and tissue engineering 2019. 11(35): p. 31605–31614.

169. Tullii G, et al., Micro-and Nanopatterned Silk Substrates for Antifouling Applications 2020. 12(5): p. 5437–5446.

170. Ganjian M, et al., Nature helps: toward bioinspired bactericidal nanopatterns 2019. 6(16): p. 1900640.

171. Xu L-C, et al., Inhibition of bacterial adhesion and biofilm formation by dual functional textured and nitric oxide releasing surfaces 2017. 51: p. 53–65.

172. Modaresifar K, et al., Bactericidal effects of nanopatterns: A systematic review 2019. 83: p. 29–36.

173. Mirzaali M, et al., In-silico quest for bactericidal but non-cytotoxic nanopatterns 2018. 29(43): p. 43LT02.

174. Gantner BN, LaFond KM, and Bonini MGJRB, Nitric oxide in cellular adaptation and disease 2020: p. 101550.

175. Yang L, et al., Nitric oxide–releasing macromolecular scaffolds for antibacterial applications 2018. 7(13): p. 1800155.

176. Pant J, et al., A multi-defense strategy: Enhancing bactericidal activity of a medical grade polymer with a nitric oxide donor and surface-immobilized quaternary ammonium compound 2017. 58: p. 421–431.

177. Estes LM, et al. , Characterization of a nitric oxide (NO) donor molecule and cerium oxide nanoparticle (CNP) interactions and their synergistic antimicrobial potential for biomedical applications. Journal of Colloid and Interface Science, 2021. 586: p. 163–177. [PubMed: 33187669]

178. Mendhi J, et al., Dose controlled nitric oxide-based strategies for antibacterial property in biomedical devices 2020. 19: p. 100562.

179. Ghalei S, et al. , Nitric oxide releasing halloysite nanotubes for biomedical applications. Journal of Colloid and Interface Science, 2021. 590: p. 277–289. [PubMed: 33548611]

180. Pant J, et al., Nitric oxide releasing vascular catheters for eradicating bacterial infection 2018. 106(8): p. 2849–2857.

181. Douglass ME, et al. , Catalyzed Nitric Oxide Release via Cu Nanoparticles Leads to an Increase in Antimicrobial Effects and Hemocompatibility for Short-Term Extracorporeal Circulation. ACS Applied Bio Materials, 2019. 2(6): p. 2539–2548.

182. Singha P, et al., Multipronged approach to combat catheter-associated infections and thrombosis by combining nitric oxide and a Polyzwitterion: a 7 day in vivo study in a Rabbit Model 2020. 12(8): p. 9070–9079.

183. Homeyer KH, et al. , Liquid-Infused Nitric-Oxide-Releasing Silicone Foley Urinary Catheters for Prevention of Catheter-Associated Urinary Tract Infections. ACS Biomaterials Science & Engineering, 2019. 5(4): p. 2021–2029. [PubMed: 33405516]

184. Homeyer KH, et al., S- Nitroso- N- acetylpenicillamine impregnated endotracheal tubes for prevention of ventilator- associated pneumonia 2020. 117(7): p. 2237–2246.

185. Ghalei S, et al. , Synergistic Approach to Develop Antibacterial Electrospun Scaffolds Using Honey and S-Nitroso-N-acetyl Penicillamine. ACS Biomaterials Science & Engineering, 2021. 7(2): p. 517–526. [PubMed: 33397083]

186. Hopkins SP, et al. , Electrospun Bioabsorbable Fibers Containing S-Nitrosoglutathione for Tissue Engineering Applications. ACS Applied Bio Materials, 2020. 3(11): p. 7677–7686.

187. Choi M, et al., Chitosan-based nitric oxide-releasing dressing for anti-biofilm and in vivo healing activities in MRSA biofilm-infected wounds 2020. 142: p. 680–692.

188. Pant J, et al. , Antibacterial and Cellular Response Toward a Gasotransmitter-Based Hybrid Wound Dressing. ACS Biomaterials Science & Engineering, 2019. 5(8): p. 4002–4012. [PubMed: 33443422]

189. Liang H, et al., Nitric oxide generating/releasing materials 2015. 1(1).

190. Brisbois EJ, et al., Long-term nitric oxide release and elevated temperature stability with S-nitroso-N-acetylpenicillamine (SNAP)-doped Elast-eon E2As polymer 2013. 34(28): p. 6957–6966.

191. Howlin RP, et al., Low-dose nitric oxide as targeted anti-biofilm adjunctive therapy to treat chronic Pseudomonas aeruginosa infection in cystic fibrosis 2017. 25(9): p. 2104–2116.

192. Simionescu B and Ivanov DJHBB, Natural and synthetic polymers for designing composite materials 2016: p. 233–286.

193. Ghalei S, et al., Silk Nanoparticles: A Natural Polymeric Platform for Nitric Oxide Delivery in Biomedical Applications 2020. 12(48): p. 53615–53623.

194. Ghalei S, et al., Silk Nanoparticles: A Natural Polymeric Platform for Nitric Oxide Delivery in Biomedical Applications 2020.

195. Grassi L, et al., Combination Strategies to Enhance the Efficacy of Antimicrobial Peptides against Bacterial Biofilms 2017. 8(2409).

196. Shang D, et al., Synergistic Antibacterial Activity of Designed Trp-Containing Antibacterial Peptides in Combination With Antibiotics Against Multidrug-Resistant Staphylococcus epidermidis 2019. 10(2719).

197. Choudhury AJ, et al., Penicillin impregnation on oxygen plasma surface functionalized chitosan/ Antheraea assama silk fibroin: Studies of antibacterial activity and antithrombogenic property 2016. 60: p. 475–484.

198. Patil PP, et al., Hybrid chitosan-ZnO nanoparticles coated with a sonochemical technique on silk fibroin-PVA composite film: A synergistic antibacterial activity 2019. 122: p. 1305–1312.

199. Pankongadisak P and Suwantong O.J.I.j.o.b.m., Enhanced properties of injectable chitosan-based thermogelling hydrogels by silk fibroin and longan seed extract for bone tissue engineering 2019. 138: p. 412–424.

200. Zhou W, et al., Bioinspired and biomimetic AgNPs/gentamicin-embedded silk fibroin coatings for robust antibacterial and osteogenetic applications 2017. 9(31): p. 25830–25846.

201. Vieira D, et al., Electroceutical Silk–Silver Gel to Eradicate Bacterial Infection 2020. 4(4): p. 1900242.

202. Ramadass SK, et al., Type I collagen peptides and nitric oxide releasing electrospun silk fibroin scaffold: A multifunctional approach for the treatment of ischemic chronic wounds 2019. 175: p. 636–643.

203. Zhou W, et al., Construction of self-defensive antibacterial and osteogenic AgNPs/gentamicin coatings with chitosan as nanovalves for controlled release 2018. 8(1): p. 1–12.

204. Yan J, et al., Endowing polyetheretherketone with synergistic bactericidal effects and improved osteogenic ability 2018. 79: p. 216–229.

205. Wenhao Z, et al., In vitro and in vivo evaluation of structurally-controlled silk fibroin coatings for orthopedic infection and in-situ osteogenesis 2020. 116: p. 223–245.

206. Gulka CP, et al., A novel silk- based vocal fold augmentation material: 6- month evaluation in a canine model 2019. 129(8): p. 1856–1862.

207. Gholipourmalekabadi M, et al., Silk fibroin for skin injury repair: where do things stand? 2020. 153: p. 28–53.

208. Holland C, et al., The biomedical use of silk: past, present, future 2019. 8(1): p. 1800465.

209. Hasatsri S, et al., Randomized clinical trial of the innovative bilayered wound dressing made of silk and gelatin: safety and efficacy tests using a split-thickness skin graft model 2015. 2015.

210. Fregnan F, et al., Preclinical validation of SilkBridgeTM for peripheral nerve regeneration 2020. 8: p. 835.

Highlights

- An overview of silk fibroin structure-properties relationship as a leading-edge biomaterial.

- A comprehensive summary of different approaches for development of antibacterial silk fibroin-based biomaterials, their fabrication methods, and biomedical applications.

- Addressing the advantages and drawbacks of each antibacterial approach and identifying the emerging trend for future research.
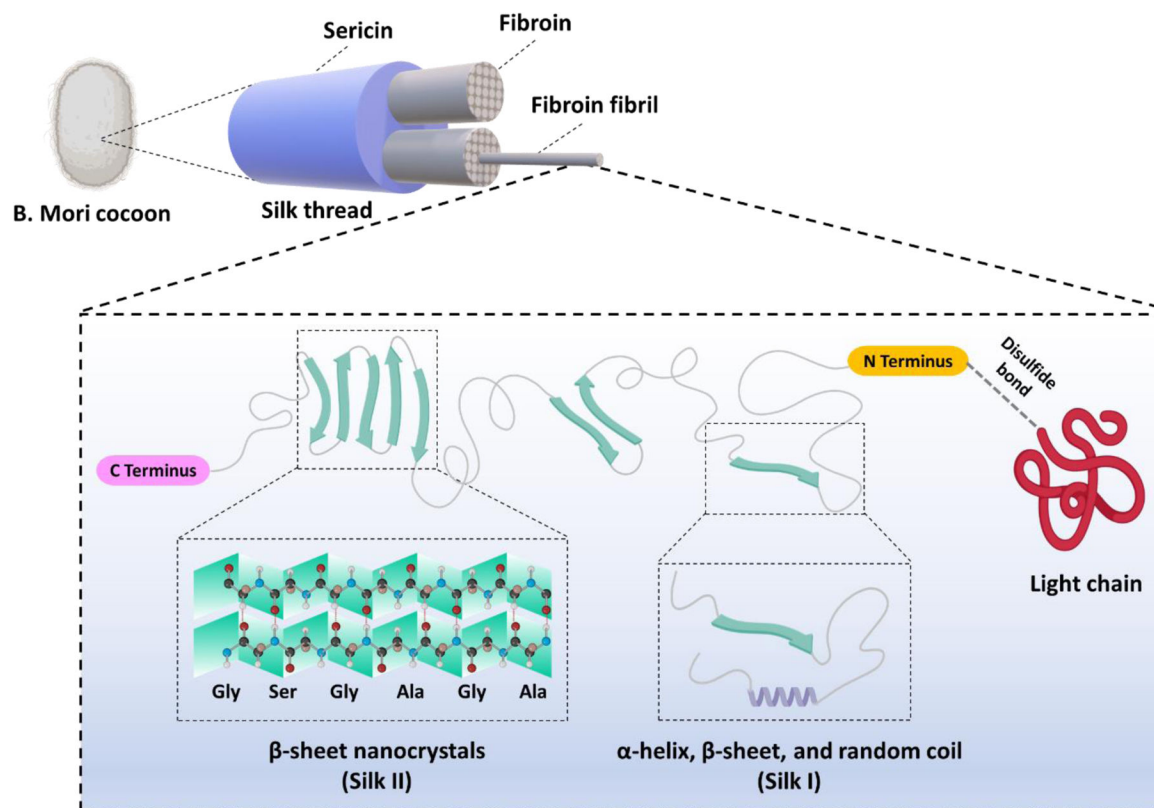
Figure 1.
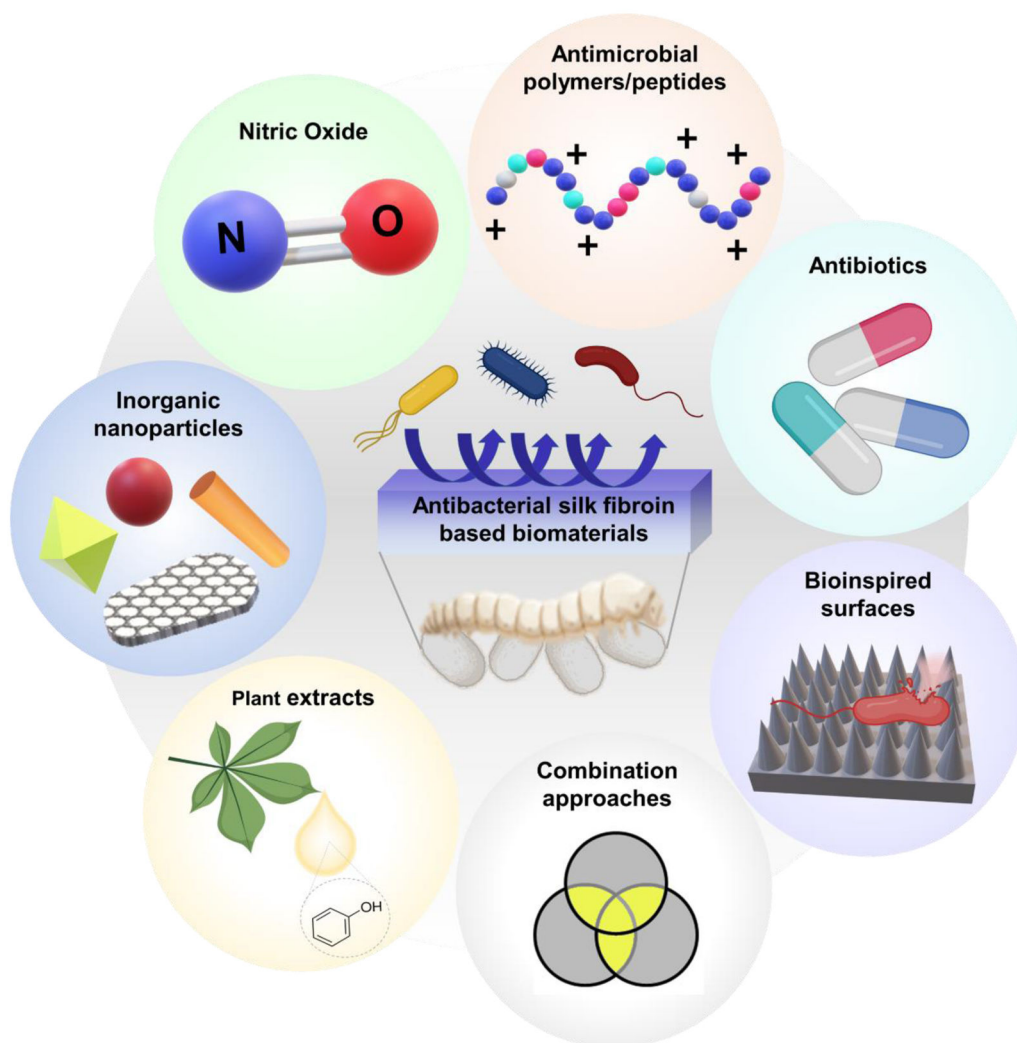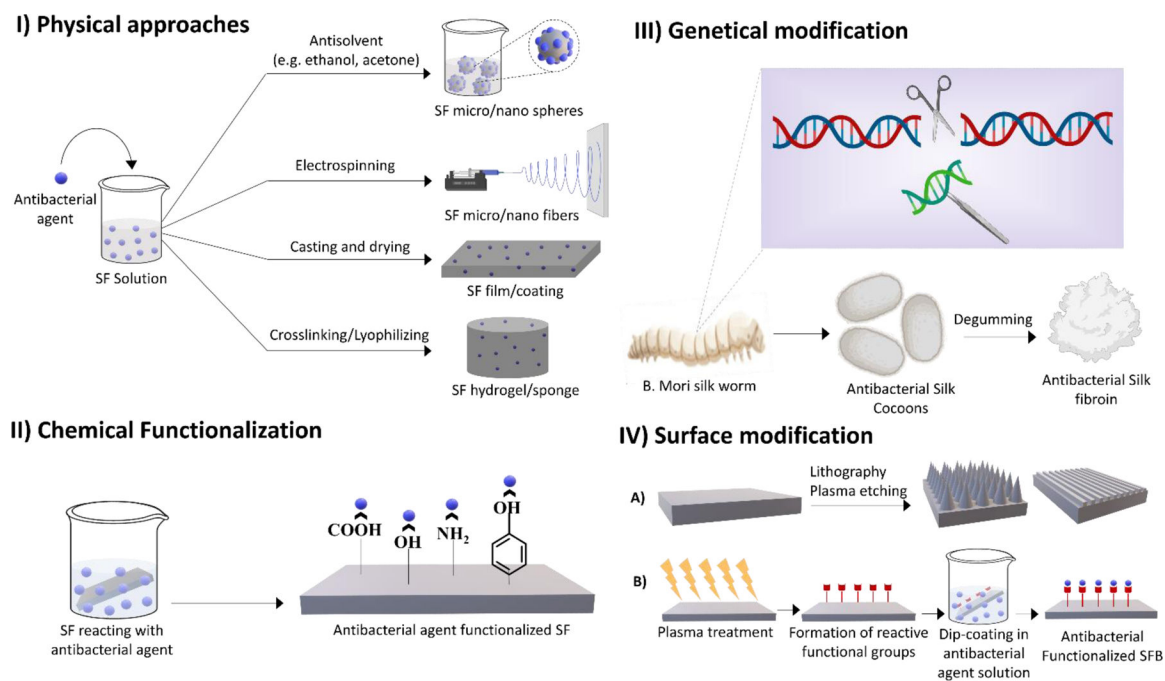A schematic representation of the B. mori silk fibroin structure

Figure 2.
Silk fibroin properties, different formats, and biomedical applications

3. Antibacterial approaches for silk-fibroin based biomaterials

Figure 3.
Different antibacterial approaches for silk fibroin based biomaterials

Figure 4.
Different methods of developing antibacterial silk fibroin based biomaterials

Table 1.

Processing and antibacterial activity of SFBs combined with antibiotics for different biomedical applications

Antimicrobial additive (antibiotics)	Other additive(s)	Synthesis method	Content	Antimicrobial capability	Application	Refs
Amoxicillin trihydrate	Chitosan	Oxygen plasma treatment and dip-coating	25 wt%	ZOI (25 d): S. aureus (5–35 mm) E. coli (15–35 mm)	Surgical suture	[48]
Amoxicillin trihydrate (AMOX)	----	Oxygen plasma treatment and dip-coating	50 µg/mL	ZOI (24 h): S. aureus (54.7 mm) E. Coli (19.3 mm) Skin infection reduction in mouse models (after 3–14 d)	Suture/wound healing	[49]
Ciprofloxacin hydrochloride	----	Molded hydrogels	9 mg/mL	Killing and growth inhibition of M. catarrhalis after 24 h (quantitative data N/A)	Bioresorbable drug-eluting ear tubes	[56]
Colistin	----	SF membranes	Log-scale dilutions (0.027–270 mg/mL)	RE (24 h): P. aeruginosa (complete elimination at 270 mg/mL) CFU (3 d) rat burn infection: >3 log	Wound dressing Biodegradable scaffold	[43]
Gentamicin	----	Electrophoretic deposition of gentamicin-loaded SF coatings on 3D-printed CoCrMo bone substitutes	1 mg/mL	ZOI (7 d): S. aureus (18–22 mm)	Orthopedic implants	[50]
Gentamicin (Gen)	Titanium (Ti) foil	Gen loaded SF NPs deposited on chemically activated Ti foil	0.1–0.3 wt%	ZOI (5–120 min): S. aureus (Diameter N/A) Reduced bacterial adhesion	Metal based implants	[57]
Gentamycin sulfate (GS)	Gelatin microspheres	GS-loaded gelatin microspheres embedded in freeze-dried SF scaffolds	10 wt%	ZOI (24 h): S. aureus (8.8 mm) E. Coli (7.5 mm) Burn infection reduction (21 d): P. aeruginosa	Treatment of infected full-thickness burns	[47]
Gentamicin sulphate (GS)	Dextrose	Dextrose incorporated muga and tasar SF films impregnated with GS	20–25 mg/samples	ZOI (24 h): S. aureus (19–21 mm) E. Coli (16–18 mm)	Wound dressing	[44]
Gentamicin sulfate (GS)	----	Molded SF-GS hydrogel screws	1.6 wt%	ZOI (24 h): S. aureus (22.2 mm) E. Coli (22.6 mm) RE (4 weeks): S. aureus (97.8 ± 3.9%) E. coli (93.4 ± 7.9%)	Absorbable fixation screw	[58]
Levofloxacin (LV)	Hyaluronic acid (HA)	i) Complex coacervate and ii) LBL deposition of LV blended HA and SF coatings on CoCrMo alloy	0.750 µg/mL	RE (24 h- Complex coacervate): S. aureus (70%) RE (24 h-LBL deposition): S. aureus (30%) SEM (24 h): Reduction in S. aureus biofilm formation	Orthopedic implants	[52]

Antimicrobial additive (antibiotics)	Other additive(s)	Synthesis method	Content	Antimicrobial capability	Application	Refs
Tetracycline hydrochloride	Halloysite nanotube	Electrospinning	2 wt%	ZOI (24 h-7 d): *S. aureus* (24.2 mm-12.8 mm) *E. Coli* (26.8 mm-12.9 mm)	Wound dressing	[53]
Tetracycline (TC)	Titanium (Ti)	Electrophoretic deposition of TC-modified SF coatings on Ti surfaces	0.15 v/v	ZOI (24 h): *S. aureus* (35 mm) *E. Coli* (20 mm)	Drug delivery of Ti implants	[51]
Vancomycin hydrochloride	Short-stranded poly (L-lactide) fibers Pectin	Electrospun fibers/hydrogel composite	3 wt%	ZOI (24 h): *MRSA* (20.3 mm)	Drug delivery Bone TE	[59]
Vancomycin (VANCO)	Gelatin microspheres	VANCO-loaded gelatin microspheres embedded in freeze-dried SF scaffolds	10 % w/w	ZOI (24 h): *S. aureus* (6.65 mm) No inhibition zone against *E. coli*	Burn and ulcer treatment	[41]
Vancomycin (VANCO)	Gelatin nanospheres	Colloid-electrospinning	0.4 wt%	ZOI (24 h): *S. aureus* (Diameter N/A)	Drug delivery system	[45]
Vancomycin (VANCO)	----	VANCO loaded SFNPs embedded in freeze-dried SF scaffolds	18.8 wt%	ZOI (26 d): *S. aureus* (11–14 mm) Reducing infection in rats with severe osteomyelitis after 6-weeks implantation	Treatment of osteomyelitis	[46]

RE, reduction efficiency; TE, tissue engineering; LBL, layer by layer; *M. catarrhalis*, *Moraxella catarrhalis*; MRSA, *Methicillin-resistant Staphylococcus aureus*; *P. aeruginosa*, *Pseudomonas aeruginosa*; MIC, minimum inhibitory concentration; CFU, colony forming unit

Table 2.

Processing and antibacterial activity of SFBs combined with inorganic nanoparticles for different biomedical applications

Antimicrobial additive (Inorganic nanoparticles)	Other additive(s)	Synthesis method	Content	Antimicrobial capability	Application	Refs
AgNPs	-----	Reduction of Ag ions by SF solution using a microfluidic device	125 μg/mL AgNO$_3$	Live/dead assay: Maximum bacterial death at 3 h; RE (2 h): E. coli (>75%) in an infected mouse model	Surgical site infections	[65]
AgNPs	Polylactic acid (PLA) Nano hydroxyapatite (nHA) Polydopamine (PDA)	Reduction of Ag ions by SF and fabrication of SF/Ag/nHA/PLA composites	50 mM AgNO$_3$ solution	Turbidity test against E. coli and S. aureus (24 h): Lower absorbance of the medium containing the scaffolds	Bone TE	[67]
Ag NPs	-----	SF as the reducing and stabilizing agent for preparation of SF-AgNPs solutions under light	0–153.6 mg/L	MRSA: MIC (19.2 mg/L) MBC (76.8 mg/L) CLSM and SEM (10 h): No biofilm formation at concentrations higher than MIC	General biomedical applications	[66]
AgNPs	-----	Dip-coating Tasar SF nanofibrous mats in AgNPs solution	1 mM AgNO$_3$ solution	ZOI (12 h): S. aureus (10 mm) E. coli (14mm) P. aeruginosa (8 mm) S. epidermidis (10 mm)	Skin TE	[78]
AgNPs	-----	Dip-coating and microwave irradiation of SF fibers in AgNO$_3$ solution	0.5, 1 and 1.5 mmol L^{-1} of AgNO$_3$ solutions	Diffusion assay (24 h): S. aureus, M. tuberculosis, and E. coli (dose-dependent antibacterial activity)	Wound healing	[90]
Ag doped hydroxy appetite (HA) NPs	Chitosan (CS) Strontium (Sr)	Freeze-dried AgSrHA/CS/SF cryogels	-----	Turbidity test (24 h): Growth inhibition of E. coli and S. epidermidis	Bone TE	[91]
AgNPs	Strontium nanotubes (SNT) Titanium (Ti) Polydopamine (PDA)	SF/Ag coating on PDA modified SNTs (created by anodizing Ti)		Turbidity test and ZOI (24 h): Antibacterial activity against S. aureus and E. coli RE (1–5 d): S. aureus and E. coli (100–70%)	Bone TE	[92]
AgNPs	-----	The SF solution containing AgNO$_3$ was exposed to light to form SF/AgNPs films	0.1–2 % AgNO$_3$	ZOI (2 d): Antibacterial activity at 0.5–1% against S. aureus and kanamycin resistant E. coli (quantitative data N/A)	Bone TE	[93]
AgNPs	-----	In situ reduction of Ag ions and fabrication of AgNPs loaded SF gels	26.5±1.24 ppm	MIC (6±1.32 ppm) and ZOI (11±2.12mm) against S. aureus after 2 d	Wound healing	[94]
AgNPs	Carboxymethyl chitosan (CMC)	In situ synthesis of AgNPs in SF solution, and fabrication of freeze-dried AgNPs-SF-CMC sponges	AgNO$_3$ solution (0.05 wt%)	Turbidity test and ZOI (24 h): Significantly lower OD values and larger inhibition zones against S. aureus and	Wound healing	[95]

Antimicrobial additive (Inorganic nanoparticles)	Other additive(s)	Synthesis method	Content	Antimicrobial capability	Application	Refs
AgNPs	----	In situ reduction reaction between SF and silver nitrate under light	153.6 and 384 mg/L of SF-AgNPs solution	SEM (7 d): Significant reduction of S aureus biofilm at 384 mg/L of SF-NS solution compared with saline. P. aeruginosa compared to control without Ag NPs and compared to AQUACEL® Ag	Sinusitis treatment	[96]
AgNPs	----	Impregnation of silk fibers with AgNPs using in situ (AgNO$_3$ solution) and ex situ (colloidal AgNPs solution) approaches	AgNO$_3$ solution (4 mM)	Higher antibacterial activity of in situ prepared fibers after 24 h. P. aeruginosa: ZOI (3.3±0.5 mm), RE (99.9%). S. aureus: ZOI (2.4±0.4 mm), RE (95%)	Wound healing	[77]
AgNPs	----	Electrospinning SF/AgNO$_3$ solution and irradiation with UV to obtain SF/AgNPs nanofibers	0.1%, 0.5%, and 1% wt/v	No antibacterial activity at 0.1% and 0.5% against S. aureus and S. epidermidis. ZOI (24 h) at 1%: S. aureus (6.5 mm) S. epidermidis (5.6 mm) P. aeruginosa (9.3 mm)	Wound healing	[97]
AgNPs	----	Dip-coating and in situ photoreduction of Ag ions on SF sutures	0.5 wt/v % AgNO$_3$ solution	Inhibition zone against S. aureus and E. coli after 24 h (Diameter N/A). RE (24 h-bacteria in solution): E. coli (78%), S. aureus (81%) RE (24 h-adhered bacteria): E. coli (34%), S. aureus (35%)	Suture	[98]
Ag@AgCl NPs	Cellulose acetate (CA)	Photocatalytic reduction and in situ formation of Ag@AgCl NPs on SF/CA composite membranes	0.1 M AgNO$_3$ aqueous solution	ZOI (24 h): E. coli (13.99 mm) S. aureus (12.59 mm)	Antibacterial applications	[99]
AuNPs	----	Reduction of AuNPs by SF solution	0.5 mM SF-AuNPs colloidal solution	RE (24 h): E. fecalis (85.19 ± 3.24 %) S. aureus (32.34 ± 1.70 %) E. coli (77.95 ± 9.59 %) P. aeruginosa (63.38 ± 4.26 %)	Nanoparticles with antibacterial and anticancer properties	[69]
AuNPs AgNPs	Nano-hydroxyapatite (nHA)	In situ reduction of AgNPs and AuNPs by SF/nHA solution and fabrication of hydrogels	0, 0.1, 0.5 and 1% HAuCl$_4$,3H$_2$O and AgNO$_3$	Turbidity test and resazurin assay (24 h): SF/AgNPs (0.1–1 %): Antibacterial activity against MSSA, MRSA, S. epidermidis, E. coli, and P. aeruginosa SF/AuNPs (0.5%): Antibacterial activity against MSSA, MRSA, S. epidermidis, E. coli, and P. aeruginosa No antibacterial activity against S. epidermidis	Bone regeneration	[68]
Diamino-2-pyrimidinethiol-functionalized Au NPs (DAPT-Au NPs)	----	Aqueous SF/Au-DAPT membranes	27 µg/cm^2	MIC and ZOI (20 h): E. coli and MDR E. coli (4 µg/mL, ~14 mm) Inhibition of growth after 20 h.	Wound healing	[100]

Antimicrobial additive (Inorganic nanoparticles)	Other additive(s)	Synthesis method	Content	Antimicrobial capability	Application	Refs
Ca^{2+}	Polyethylene glycol diglycidyl ether (PEG-DE)	Freeze-dired Ca^{2+} loaded SF-PEG-DE porous material	1.8, 3.6, 5.4, and 7.2%, (w/w)	CFU and turbidity test (6 h): Inhibitory effect on the bacterial growth and propagation of *E. coli* and *S. aureus*	Hemostatic material	[86]
Calcium peroxide (CPO)	Gelatin (GL) Human keratin (HK)	Physical blending to make composite film scaffolds	20% CPO	ZOI (24 h): *E. coli* (3.55 ± 0.24 mm) *S. aureus* (2.89 ± 0.20 mm)	Urethral TE	[87]
CuBTC MOF particles	-----	Formation of CuBTC MOF on silk yarns by immersing in $Cu(OAc)_2.2H_2O$, and H3BTC solution	2–8 dipping cycles	ZOI (24 h- IV-cycle 4): *E. coli* (7.7 mm) *S. aureus* (6.5 mm) ZOI (24 h- IV-cycle 10): *E. coli* (8.0 mm) *S. aureus* (7.5 mm)	Wound healing and medical applications	[70]
Graphene oxide (GO)	-----	Electrospining	5 wt% GO	Survival rate after 18 h: *E. coli* (35.7 ± 3.6 %) *S. aureus* (41.6 ± 0.3%) SEM: Shrunken morphology of *E. coli* on the SF/GO nanofibers	Wound dressing	[80]
Graphene oxide (GO) Reduced GO (RGO) Graphene (Gr)	-----	Electrospinning	1 wt%	RE (24 h): Antibacterial activity of SF/GO, SF/RGO, and SF/Gr against *S. aureus* (92.8%, 98.6%,80.6%) and *E. coli* (70.3%, 84.9%, 69.5%)	TE	[101]
Reduced Graphene oxide (GO) TiO_2	-----	Electrospinning	0.01 wt%	RE against *S. aureus*: SF/RGO: 94.8% SF/TiO_2: 83.6% SF/GO/TiO_2: 84.9%	TE	[102]
$MgOH_2$ nanorods	Polyvinyl alcohol Sodium Alginate	Freeze-dried Hydrogels	0.3 wt%	Crystal violet assay (24 h): Inhibition of *P. aeruginosa* biofilm formation	TE and general biomedical applications	[103]
$MoSe_2$ nanosheets	-----	Exfoliation of $MoSe_2$ nanosheets by carboxyl-modified SF (CMSF) solution	$MoSe_2$–CMSF nanosheets (50 μg mL^{-1})	Live/dead assay, SEM, turbidity test, and CFU (6 h): Antibacterial activity against *E. coli* and *B. subtilis*	Wound dressing	[76]
TiO_2	-----	TiO_2/SF blend membranes	TiO_2/SF weight ratios: 1/1000, 3/1000, 5/1000, and 10/1000	1/1000 samples showed the highest antibacterial activity ZOI (24 h): *S. aureus* (19.0±0.2) *E. coli* (17.0±0.1) *P. aeruginosa* (13.0±0.2)	Skin TE and wound dressing	[85]
TiO_2	Chitin (Ch) Glycerol (Gly)	Freeze-dried SF/Ch/TiO_2 wound dressings	0.5, 1.5, 3.0 % (w/w) TiO_2	ZOI (24 h): *S. aureus* (19 mm) *E. coli* (20–22 mm) CFU (3% TiO_2): 5-fold decrease in number of colonies	Wound dressing	[84]

Antimicrobial additive (Inorganic nanoparticles)	Other additive(s)	Synthesis method	Content	Antimicrobial capability	Application	Refs
ZnO NPs	Sodium alginate (SA)	Dip-coating SF fibers functionalized with SA in ZnO NPs solution	0.5% suspension of ZnO NPs	ZOI (2–6 d): *S. aureus* (1.9–0.5 mm)	Suture	[83]
ZnO NPs	Hyaluronic acid (HA)	Co-axial electrospinning	1, 3, and 5% w/v ZnO NPs	ZOI (24 h) (5% ZnO fibers): *E. coli* (2.93±0.12 mm) *S. aureus* (3.37±0.12 mm) CFU (24 h): *E. coli* (28±2 colonies) *S. aureus* (6±1 colonies)	Burn wound healing	[82]
Porous ZnO NPs (PZ)	----	Dip-coating silk thread in PZ solution	50 mM $Zn(NO_3)_2 \cdot 6H_2O$ initial solution	RE (6–8 h): *S. aureus* and *E. coli* (~80%) Suppressing bacterial infection in a mouse model (2 w)	Suture	[81]

MDR, multi drug resistanat; MSSA, *methicillin-susceptible Staphylococcus aureus*; *S. epidermidis, Staphylococcus epidermidis*; MBC, minimum bactericidal concentration; SEM, scanning electron microscopy; CLSM, confocal laser scanning microscopy

Author Manuscript

Author Manuscript

Author Manuscript

Author Manuscript

Table 3.

Processing and antibacterial activity of SFBs combined with inherently antimicrobial polymers and peptides for different biomedical applications

Antimicrobial additive (polymers and peptides)	Other additive(s)	Synthesis method	Content	Antimicrobial capability	Application	Refs
Carboxymethyl chitosan (CMC)	-----	LBL CMC coating on electrospun SF nanofibers	1mg/ml (1–21 layers)	RE (12 h) and SEM: *E. coli* (64%) *S. aureus* (67%)	TE	[131]
Chitosan (CS)	Egg shell membrane (ESM)	CS/SF/ESM hydrogels	2% w/v	ZOI (time N/A): *E. coli* (39 mm) *Candida albicans* (42 mm)	Cartilage TE	[132]
Chitosan (CS)	Nylon6 (N6)	LBL deposition of CS and SF on N6 nanofibrous mats	1 mg/mL (5–20 layers)	RE (16 h) *E. coli* and *S. aureus* (> 95%)	Pelvic floor reconstruction	[133]
Chitosan (CS)	Heparin	Heparinized SF blended with CS	2% w/v	Significant inhibitory effect on *S. aureus* proliferation compared to samples without CS.	Blood contacting devices	[134]
Chitosan (CS)	Transforming growth factor-β (TGF-β)	UV-crosslinked methacrylated SF NPs with CS	6 wt%	RE (24 h): *E. coli* (83%) *S. aureus* (67%)	Articular Cartilage TE	[135]
Chitosan (CS)	Polycaprolactone (PCL) Heparin (Hep)	LBL deposition of Hep/CS on PCL/SF nanofibers	1mg/ml (1–10 layers)	RE (16 h): *E. coli* and *S. aureus* (up to 95%)	Vascular grafts	[136]
Chitosan (CS)	-----	Electrospining	CS/SF blend fibers: (80/20); (50/50); (20/80); (0/100)	Turbidity test (24 h): *E. coli* (increased antibacterial activity with increased CS content)	Wound dressing	[137]
Chitosan (CS)	-----	Freeze-dried CS/SF scaffolds	The SF/CS blend ratios: 2:1, 1:1, 1:2, and 1:3	Turbidity test (24 h): *S. aureus* (higher antibacterial activity of 1:2 and 1:3 samples) SEM (24 h): *S. aureus* (fewer adherence on blended samples)	TE	[138]
Chitosan (CS)	Rectorite (REC)	LBL deposition of CS and REC on SF electrospun mats	16 CS and 15 REC layers (1 mg/mL)	RE (24 h): *E. coli* (84%) *S. aureus*, (92%)	Bone TE	[139]
Chitosan (CS)	Polydopamine (PDA)	LBL CS/PDA coatings on SF nanofibers	15 layers of CS (1 mg/mL) and PDA on 2 cm² SF mats	RE (24 h): *E. coli* and *S. aureus* (~ 98%)	General biomedical application	[140]
Chitosan (CS)/ Polydopamine nanoparticles (PDA NPs)	-----	Freeze-dried SF/CS/PDA cryogels	-----	Enhanced antibacterial activity against *E. coli* and *S. aureus* (quantitative data N/A)	Wound healing	[141]
Chitosan NPs (NCS)	Hyaluronic acid (HA)	Freeze-dried NCS/HA/SF scaffolds	5% CS solution	ZOI (24 h): *E. Coli* (16 mm) *Pseudomonas aureus* (14 mm)	TE	[142]
Chitooligosaccharide (COS)	-----	Enzymatic grafting of COS onto SF membranes	-----	RE (24 h): *E. coli* (87.62%)	General biomedical application	[143]

Antimicrobial additive (polymers and peptides)	Other additive(s)	Synthesis method	Content	Antimicrobial capability	Application	Refs
Quaternized chitin	Polycaprolactone (PCL)	LBL deposition of QC and SF on SF/PCL electrospun mats	7 layers of QC (1 wt%)	RE (5 h): Higher antibacterial activity against *S. aureus* than *E. coli* (93.63 ± 2.09%) a	Skin TE	[144]
Polyethyleneimine	Polymethyl methacrylate	Electrospinning	1% w/v	ZOI (24 h): *P. aeruginosa* (Diameter N/A)	Dental applications	[145]
Polyethyleneimine	-----	Electrospinning	10, 20 and 30% w/w	Complete inhibition of *S. aureus* and *P. aeruginosa* growth after 5 h	Wound dressing	[108]
Poly(hexamethylene biguanide)hydrochloride (PHMB)	-----	Freeze-dried SF/PHMB sponges	PHMB/SF ratios: (0/100–10/100)	ZOI (24 h): *E. coli* and *S. aureus* inhibition zone at >2/100 ratios (Diameter N/A)	Wound healing	[110]
Polypropylene (PP)	-----	PP grafted Muga SF sutures fabricated by argon plasma graft polymerization	-----	ZOI (24 h): *E. coli* (35±0.01 mm)	Suture	[109]
Human neutrophil defensin 2 (HNP-2), human neutrophil defensins 4 (HNP-4), and hepcidin fusion peptides	-----	Cloning and fusing spider silk	10, 50 and 100 µg/mL protein solutions	ZOI (24 h): *E. coli* and *S. aureus* (highest bactericidal activity for HNP-4 and lowest bactericidal activity for HNP-2)	TE	[123]
6mer-HNP1 antimicrobial peptide	-----	Dip coating silk sutures (Perma-Hand®)	2 wt%	CFU (24 h): MRSA (~1.5 log) *E. coli* (~2 log)	Suture	[117]
HPRP-A2 antimicrobial peptide	-----	Electrospinning	0.01% (wt/v)	RE (18 h): *E. coli* (90.39%) *P. aeruginosa* (72.93 %) *S. aureus* (98.19 %) *S. epidermidis* (72.05 %)	Wound Dressing	[118]
Antimicrobial peptide motif (Cys-KR12)	-----	Cys-KR12 immobilization onto electrospun SF mats using EDC/NHS and thiol-maleimide click chemistry	0.15–1.43 nmol per square centimeter	RE (4h): Strong antibacterial properties against *S. epidermidis*, *E. coli*, and *P. aeruginosa* (>3 log) SEM: No biofilm formation after 24 h	Wound healing	[120]
Cecropin B (CB) antimicrobial peptide	-----	CB modified SF films by carbodiimide chemistry	-----	RE (24 h): *E. coli* (93.5%) *S. aureus* (91.6%)	Implantable biomaterials	[119]
L-Cysteine (L-Cys)	-----	Covalent immobilization of L-Cys on SF knitted fabric	-----	RE (24 h): High bactericidal efficiency against *S. aureus* at both acidic pH (78.4–89.3 %) and basic pH (77.3–98.6 %)	Skin disease management	[121]
e-polylysine (e-PLL)	-----	enzymatic oxidization of SF with tyrosinase followed by coupling of e-PLL	-----	CFU (18 h): *S. aureus* (~1.97 log)	General biomedical application	[122]

Antimicrobial additive (polymers and peptides)	Other additive(s)	Synthesis method	Content	Antimicrobial capability	Application	Refs
ε-polylysine (PLS) Chitosan (CS)	-----	SF/PLS/CS bioadhesive composite	10 wt% CS/PLS	ZOI (120 min): *S. aureus* (10.2 mm) *E. coli* (10.4 mm)	Wound healing	[146]
Quaternary ammonium compound (QAC-K21)	-----	Dip-coating silk suture strips	5%, 10%, 20%, and 25% K-21 solutions	ZOI (12 d): Inhibition zone against *P. gingivalis* and *E. faecalis* for 25% solution	Suture	[125]

Table 4.

Processing and antibacterial activity of SFBs combined with plant extracts for different biomedical applications

Antimicrobial additive (Plant extracts)	Other additive(s)	Synthesis method	Content	Antimicrobial capability	Application	Refs
Chinese herbal extract (Baicalein, BAI)	Polyvinylpyrrolidone (PVP)	Electrospinning	18 wt % BAI	RE (24 h): *S. aureus* (88.2–98.9%) Reduction of infection in a wound mouse model (0–25 d)	Wound healing	[154]
Elaeagnus Angustifolia	polyvinyl alcohol	Electrospinning	10 v/v%	RE (24 h): *S. aureus* (99.5±0.3 %) *E. coli* (99.2±0.4%)	Wound dressing	[155]
Manuka honey (MH)	-----	Electrospinning Methanol crosslinked cryogels	5% of MH with 5 and 20 unique manuka honey factor (UMF)	ZOI (24 h-cryogels): *E. coli* and *S. aureus* (~ 0.16 cm) ZOI (24 h-nanofibers): *E. coli* and *S. aureus* (0.5–1 cm) CFU and SEM (4 h-adhered bacteria): Significant reduction of bacteria compared to control	Treatment of chronic bone infections	[156]
Manuka honey (MH)	Polyethylene oxide (PEO)	Electrospinning	0, 10%, 30%, 50% and 70% (wt/v) MH (UMF 5⁺)	ZOI (18 h-SF/MH(70%)): *E. coli* (7.6 mm), *S. aureus* (4.5 mm), *P. aeruginosa* (8.3 mm), and MRSA (6.7 mm) RE measured by turbidity test (24 h): *E. coli* (51%), *S. aureus* (29%), *P. aeruginosa* (57%), and MRSA (40%)	Wound dressing	[157]
Nigella sativa (NS)	-----	Electrospinning	1 and 1.5 % NS	ZOI (24 h-SF/NS1%): *E. coli* (8mm) and *S. aureus* (12mm) ZOI (24 h-SF/NS1.5%): *E. coli* (10mm) and *S. aureus* (14mm)	General biomedical application	[158]
Olive leaf extract (OLE)	Hyaluronic acid (HA)	Co-axial electrospinning	12 and 15% (w/v) OLE	RE (0–1 h): *S. aureus* and *E. coli* (99.98–100.00%)	General biomedical application	[159]
Oregano essential oil (OEO)	Poly (L-lactide-co-caprolactone) (PLCL)	Electrospinning	2.5 and 5 v/v%	Turbidity test RE (24 h): *S. aureus* (93.93±1.23 – 100±0.61%) *E. coli* (52.91±1.48 – 98.02±0.34%) ZOI against *S. aureus* and *E. coli* after 24 h (*quantitative data N/A*)	Wound dressing	[160]
Pistacia terebinthus (PT), *Pistacia lentiscus* (PL), *and Hypericum empetrifolium* (HE)	Chitosan (CS)	Dip-coating SF/CS blend films in different plant extracts	0.05 g of films soaked in 2 mL of 4% (w/v) PT, PL, and HE extracts	Turbidity test (24 h): Growth inhibition of *E. coli* and *S. epidermidis*	Wound healing	[161]
Thymol (THY)	Polycaprolactone (PCL) Hyaluronic acid (HA)	Electrospinning	5 mg/mL THY	RE and SEM (24 h): *S.aureus* (87.42%) and *P.aeruginosa* (58.43%) No biofilm formation	Wound dressing	[162]
Vanillin (V)	Keratin (K)	SF/K/V freeze-dried scaffolds	20 mM	ZOI and RE (24 h): *E. coli* (93.3%)	Skin TE	[163]

Author Manuscript

Author Manuscript

Author Manuscript

Author Manuscript

Antimicrobial additive (Plant extracts)	Other additive(s)	Synthesis method	Content	Antimicrobial capability	Application	Refs
				S. aureus (68.4%) > 50% reduction efficiency after 48 h.		

Table 5.

Processing and antibacterial activity of SFBs developed through bioinspired approaches for different biomedical applications

Antimicrobial additive (Bioinspired)	Other additive(s)	Synthesis method	Content	Antimicrobial capability	Application	Refs
Micro-nano patterns	------	Soft lithography	Nanostrips and microwell morphologies	Fluorescent imaging and turbidity test (24 h): 66% decrease in the number of adhered *E. coli*	Antifouling biomaterials	[169]
Nanopatterns	------	oxygen plasma etching	Homogeneous nanocones	SEM and live/dead assay (6–24 h): Reduced attachment of *E. coli* and *S. aureus* bacteria (>90%)	Orthopedic implants and TE	[168]
S-Nitroso-*N*-acetylpenicillamine (SNAP)	------	SNAP loaded SF NPs synthesized by an antisolvent method	9.1 ± 0.6% (w/w) SNAP	RE (24 h- 0.25 to 10 mg/mL): MRSA (48.17 to 99.99%) *E. coli* (53.77 to 99.96%)	General biomedical application	[194]

Table 6.

Processing and antibacterial activity of SFBs combined with multiple antibacterial agents for different biomedical applications

Antimicrobial additive (Combination)	Other additive(s)	Synthesis method	Content	Antimicrobial capability	Application	Refs
AgNPs Gentamicin (Gen)	Titanium (Ti) Polydopamine (PD)	Dip coating Ti implants with SF/AgNPs/Gen solutions	$AgNO_3$ (2–120 mM/L) Gen (200–1200 μg/L)	MIC against *S. aureus*: SF/AgNPs (>120 mM/L) SF/Gen (1000–1200 μg/L) SF/AgNPs/Gen (Removal of all bacteria at Gen (200 μg/L) and Ag^+ (10 mM/L)) RE of adhered bacteria after 24 h (>95%)	Osteogenetic applications	[200] [203] [204, 205]
AgNPs Electric current	-----	*In situ* reduction of Ag^+ by SF and fabrication of SF/AgNPs gels	0%, 5%, 10%, 25%, and 50% (w/w) $AgNO_3$ with electric current of 1.5 S cm^{-1}	RE (1 min-50% $AgNO_3$): *E. coli* (80%)	Wound healing	[201]
Chitosan (CS) Penicillin (PEN)	-----	Oxygen plasma treatment of *Antheraea assama* SF yarn and functionalization with CS and PEN	CS (760 ± 6 μg) on each yarn (90 cm) PEN (25–250 μg)	ZOI (24 h): *B. subtilis* (30.2±0.4 mm) *E. coli* (6.3±0.4 mm)	Blood-contacting biomaterials	[197]
Chitosan (CS) Water crude longan seed extract (WLS)	-----	CS/SF/WLS injectable hydrogels	----	RE (2 h): *E. coli* (100%) *S. aureus* (86%)	Bone TE	[199]
Chitosan (CS) ZnO	Polyvinyl alcohol (PVA)	Dip-coating SF/PVA composite films in CS-ZnO NPs solution	0.2, 0.5, and 1 wt% Cs-ZnO NPs	ZOI (24 h-1 wt%): *S. aureus* (4 mm), *E. coli* (5 mm), and *P. mirabilis* (4 mm)	Wound dressing	[198]
Type I collagen peptide (CP) *S*-Nitrosoglutathione (GSNO)	Polyvinyl alcohol (PVA)	Electrospinning	1% and 0.5% (w/v) of GSNO and CP	ZOI (24 h-CP/SF/PVA): *E. coli* (18 ± 0.28 mm) *P. aeruginosa* (17 ± 0.31 mm) *S. aureus* (9 ± 0.16) ZOI (24 h-CP/GSNO/SF/PVA) *P. aeruginosa* (22 ± 0.24) *S. aureus* (20 ± 0.27) *E. coli* (23 ± 0.19)	Treatment of ischemic chronic wounds	[202]